

國立交通大學

生物科技學系

碩士論文



比較不同奈米金球在電極表面修飾的模式於過
氧化氫的反應

**Comparison of Different Surface Modifications of Electrode
with Gold Nanoparticles in Detection of Hydrogen Peroxide**

研究生：黃啟彥

指導教授：袁俊傑 博士

中華民國 102 年 1 月

比較不同奈米金球在電極表面修飾的模式於過氧化氫的反應

Comparison of Different Surface Modifications of Electrode with Gold

Nanoparticles in Detection of Hydrogen Peroxide

研究生：黃啟彥

Student : Chi-Yen Huang

指導教授：袁俊傑 博士

Advisor : Dr. Chiun-Jye Yuan

國立交通大學



Submitted to Institute of Biological Science and Technology

National Chiao Tung University

In Partial Fulfillment of the Requirements for the Degree of Master

In Biological Science and Technology

Jan 2013

Hsinchu, Taiwan, Republic of China

中華民國一〇二年一月

比較不同奈米金球在電極表面修飾的模式於過氧化氫的反應

研究生：黃啟彥

指導教授：袁俊傑 博士

國立交通大學 生物科技學系(研究所)碩士班

中文摘要

在食品工業上，過氧化氫經常用於食品漂白、微生物的控制及無菌包裝上。長期食用，可能導致健康傷害。為了確認奈米金球修飾於碳膠電極表面，對於測定過氧化氫反應的影響。首先在碳膠電極表面以電化學方式，重氮化一層 4-aminophenylacetic acid (CMA)於電極表面。隨後，將奈米金球或表面已修飾過的奈米金球，以物理吸附或共價鍵結於 CMA 電極上。將奈米金球修飾後的碳膠電極，經由循環伏安法(cyclic voltammetry)、定電位測定法(current-time responses)量測溶液中過氧化氫的反應。碳膠電極、奈米金球修飾後的碳膠電極，以及半胱胺奈米金球修飾後的碳膠電極，測量出過氧化氫的電流訊號值為 7.94×10^{-6} , 1.41×10^{-5} , 1.44×10^{-5} A/cm²/mM，結果顯示奈米金球修飾後碳膠電極確實可以增加過氧化氫的電化學訊號。

Comparison of Different Surface Modification of Electrode with Gold Nanoparticles in Detection of Hydrogen Peroxide

Student : Chi-Yen Huang

Advisor : Dr. Chiun-Jye Yuan

Institute of Biological Science and Technology
National Chiao Tung University

Abstract

In the food industry, hydrogen peroxide was often used for food bleaching, microbiological control and aseptic packaging. Long-term consumption may cause health damage. To verify the effect of gold nanoparticle modification on screen-printed carbon paste electrode (SPCE) in the detection of hydrogen peroxide (H_2O_2) SPCE was first functionalized by electrochemical diazotization to deposit a layer of 4-aminophenylacetic acid (CMA) on the surface of SPCE. Subsequently, the gold nanoparticles (AuNPs) or the surface modified AuNPs were coated on top of the CMA layer by either physical absorption or covalent bonding. The capability of the gold nanoparticles-modified SPCE to detect hydrogen peroxide in solution was investigated by cyclic voltammetry and current-time responses. The sensitivity of SPCE, SPCE modified with AuNPs and cysteamine-coated AuNPs to H_2O_2 was 7.94×10^{-6} , 1.41×10^{-5} , 1.44×10^{-5} $\text{A}/\text{cm}^2/\text{mM}$. The results showed that the modification of SPCE with gold nanoparticles markedly increased the electrochemical response to H_2O_2 .

Acknowledgment

首先感謝袁俊傑老師，感激他在我碩士生涯這段時間裡始終沒有放棄過我，反而給予許多關懷與指導。因為我的個性內向，對於請教別人總是感到困難。但老師卻一直給予鼓勵與支持，讓我勇於面對問題、解決問題，而不是逃避問題。感謝俊龍學長、昭宏、蘭懿在我遇到實驗瓶頸時，總是給予我許多知識上、經驗上的幫助。林蔚學長、志彥、一飛、俊輝，感謝你們這段期間的協助，以及學弟辰翰、庭源、學妹于馨，感謝你們在我困難時的幫助。除此之外，感謝小伍給予我在經驗上的傳承與實驗上的幫助。感謝一直在我背後支持我的父母，沒有你們的堅持，就沒今天的我。以及我的女朋友瑜涵和她的家人，感謝妳們陪我渡過我最難過的日子。感謝交大的便利網路，讓我對於實驗上的問題能更快速、有效率得到相關的解答，以及 paper 的搜尋。最後感謝那些在我碩士生涯中給予幫助的人，無論是課業、實驗，甚至是生活、待人處事上，不吝回答或解決我的各種疑問。

Content

中文摘要.....	i
Abstract.....	ii
Acknowledgment.....	iii
Content.....	iv
Figure index.....	vi
1. Introduction.....	1
1.1 The characteristics and application of biosensors.....	1
1.2 Hydrogen peroxide and its determination.....	3
1.3 Surface treatment of screen-printed carbon electrode (SPCE).....	5
1.4 Diazotization and electro-addressing.....	6
1.5 Gold nanoparticles (AuNPs) and its applications.....	7
2. Materials and Methods.....	9
2.1 Materials.....	9
2.2 Apparatus.....	9
2.3 Preparation of gold nanoparticles (AuNPs).....	9
2.4 Preparation of cysteamine-modified AuNPs.....	10
2.5 Pretreatment and modification of screen-printed carbon paste electrode.....	11
2.6 Modification of CMA-coated SPCE with CNH₂AuNPs.....	12

2.7 Generation of glucose oxidase electrode	12
2.8 Cyclic voltammetry and electrochemical measurements	13
3. Results and Discussion	15
3.1 Generation and characterization of gold nanoparticles	15
3.2 Generation and characterization of cysteamine-AuNPs	15
3.3 Preparation of diazonium salt-coated SPCE	17
3.4 Characterization of AuNP-modified CMA/SPCE	18
3.5 Development and characterization of GOx electrode	19
4. Conclusion	21
5. Reference	22
Figures	34



Figure index

Figure 1. The surface modification and applications of gold nanoparticles. -----	34
Figure 2. Diagram of the modification of AuNPs with cysteamine. -----	35
Figure 3. The appearance of the synthesized AuNP colloidal with or without surface modification of cysteamine. -----	36
Figure 4. Wavelength scanning of AuNP and CNH ₂ -modified AuNPs within wavelengths between 400 and 700 nm. -----	37
Figure 5. Wavelength scanning of AuNPs with different level of CNH ₂ modification. -----	38
Figure 6. Chemical structure of aniline derivatives 4-(aminophenyl)acetic acid. ----	39
Figure 7. Simple diagram of diazotization and coupling reactions. -----	40
Figure 8. Electrodeposition of diazonium salt on the surface of SPCE by cyclic voltammetry. -----	41
Figure 9. Cyclic voltammetry of 1 mM K ₃ [Fe(CN) ₆] in pH 2.0 or pH 7.0 PBS. ----	42
Figure 10. Activation and modification of amine group of CMA on the SPCE for the immobilization of AuNPs. -----	43
Figure 11. Cyclic voltammograms of [Fe(CN) ₆] ³⁻ in PBS, pH 7.0. -----	44
Figure 12. Cyclic voltammograms of 500 μM H ₂ O ₂ in PBS, pH 7.0. -----	45
Figure 13. Current-time response of on SPCE and modified SPCE. -----	46

Figure 14. Dose response of SPCE and modified SPCE to H₂O₂. ----- 47

Figure 15. Electrochemical response of SPCE and modified SPCE. ----- 48

Figure 16. Current-time response curves of CNH₂AuNPs/CMA/SPCE. ----- 49

Figure 17. Simple diagrams of the construction of glucose biosensors. ----- 50

Figure 18. Dose responses of the developed glucoses biosensors to glucose.----- 51

Figure 19. Sensitivity of GOx/CMA/SPCE, GOx-CNH₂AuNPs mix/CMA/SPCE and
GOx/CNH₂AuNPs/CMA/SPCE to 500 μM glucose. ----- 52



1. Introduction

1.1 The characteristics and application of biosensors

The biosensors are analytical devices that use immobilized biomolecules to recognize the chemical and biological substances and convert non-electrical enzymatic responses to the electric signals, which can be detected by the underneath transducers. They consist of two key parts, the recognition element and the transducer. The recognition element is basically a biological substance that could be a protein, enzyme, receptor, antibody, nucleic acid, cell or even a tissue. The transducer is a hardware instrument component that converts biological, chemical and physical signals into electric signals [1]. Biosensors exhibit the great usage in determining serum components, metabolites, pollutants, hormones, drugs, food additives, pathogens, microbes, toxins, and many more. Biosensors exhibit many advantages over the conventional analytical methods such as quick response, high sensitivity, instant output, small sample volume, reliability, ease of use and low cost [2, 3-4].

The applications of biosensors are mainly focused on four categories: (i) Medical monitoring and clinical diagnosis: this type of biosensors are highly demanded by the clinics and health care system for the diagnosis and monitoring of the progression diseases and the therapeutic effect of medicines [5]; (ii) Bioreactor process monitoring: bioreactors are essential in fermentation industries for mass production of chemicals, biochemicals and biological substances. To better control the process it is necessary to real-time monitor some key substances generating or consuming in the this process, such as glucose, ammonia, carbon

dioxide, alcohol, antibiotics and other ingredients [6]; (iii) Environmental monitoring and protection: biosensors are suitable for monitoring the discharging of pollutants, such as toxic substances in air or water, from manufacturing factories [7, 8]; (iv) Food and Agricultural monitoring: for soil and crop pesticide residue detection and drug residues detection in meat [9, 10].

Biosensors can be divided into two main types based on the recognition element used in the development. First is the bioaffinity sensors, in which the biological components recognize target substance by interaction or shape change, which generates signals of mass change and heats (such as hormones, proteins, antigens or antibodies) [11]. The other is the biocatalysis sensors, in which the target molecules are recognized by enzymes that catalyze certain reactions, which can be converted to electric signals [12]. There are three classes of biocatalysis biosensors based on the signal generated by the catalysis, including electrochemical biosensors, optical-based biosensors and thermal biosensors. The electrochemical biosensors detect the electroactive components, the reactants or products, or ions of the enzymatic reactions in the enzymatic reactions by electrochemical responses or conductivity [13, 14]. Optical-based biosensors are fabricated to detect the emission of fluorescence or phosphorescence, ultraviolet or visible light, and the chemiluminescence or bioluminescence generated during enzymatic reactions [15-17]. Surface plasmon resonance (SPR) biosensor is another example of optical-based biosensor design, by which the

interaction between molecules can be detected. SPR is the collective oscillation of electrons on the metal thin film by the incident light photons, which exhibit frequency matching the oscillation frequency of electrons on the metal surface [18, 19]. In addition to traditional precious metals, gold nanoparticles can effectively increase the sensitivity of SPR biosensor and can also enhance SPR for biological measurement of small molecules or ions [20]. The SPR biosensor has advantages of high sensitivity, low detection limit and label-free [21]. Thermal-detecting biosensors are useful in detecting temperature changes of almost all chemical reactions, interaction between molecules and acid neutralization [22, 23].

1.2 Hydrogen peroxide and its determination

Hydrogen peroxide (H_2O_2) is one of the side products of the energy metabolism in the mitochondria [24] and is also produced by neutrophils and leukocytes to fight microorganisms, remove damaged tissues and to start the inflammation during the wound-healing process [25].

Killing the invaded microorganisms at the wound sites should buy time for the immune system to heal [26].

H_2O_2 may be used as a food additive because of its bactericidal and fungicidal activity. Interestingly, it also exhibits a bleaching effect. Therefore, H_2O_2 was popular to be used by the manufacturers to prevent the darkening of products under the normal storage conditions. Apparently, the consumers are more willing to buy foods or products with present appearance or color texture. This consuming behavior prompts manufacturers to use H_2O_2 to improve the

appearance of food or products. H_2O_2 is also one of the products of oxidases and is broadly utilized as a detection target in different areas, such as clinical diagnosis, food analysis, pharmaceutical and environmental analyses [27]. However, long-term exposure to H_2O_2 may cause a variety of lesions, such as gastrointestinal ulceration, mucosal inflammation, due to the DNA damage and gene mutations in human genome [28]. In addition H_2O_2 may accelerate the aging process of the human body and play a role in the development of senile dementia, especially Alzheimer's dementia [29].

Determination of H_2O_2 is important, because it is not only broadly used in many foods and cosmetic products, but also an essential component in pharmaceutical, clinical, industrial and environmental analyses [30]. Furthermore, it is one of electroactive substance produced in the enzymatic reactions of redox enzymes [31]. Conventionally, H_2O_2 was detected by peroxidase in the presence of various chromogens, by which the color products or chemiluminescence could be generated and detected. However, these methods are often time-consuming, highly prone to interference, and costly.

Electrochemical methods, especially the amperometric biosensor, exhibit advantages, such as simple, high efficiency and high sensitivity [32] that may overcome the above drawbacks for determination of H_2O_2 . Under the reductive potential the H_2O_2 can be reduced into H_2O and generates response currents that allow us to quantitate the amount of H_2O_2 generated in reactions. The rate of H_2O_2 generation during the enzymatic reactions may

correlate to the reaction rate of corresponding oxidases [33].

1.3 Surface treatment of screen-printed carbon electrode (SPCE)

Screen-printing carbon electrode (SPCE) was broadly adopted by manufacturers for the production of the test strips of glucose meter due to its simplicity, inexpensive and easy mass production [34]. With these characteristics a variety of the amperometric biosensors were developed for a wide variety of applications by using SPCE in the enzyme electrode preparation [35, 36].

The SPCE is generated by screen-printing the carbon ink that contains ultrafine graphite powder, organic oil, pasting binder and other minor reagents, onto a solid support. However, the surface of the SPCE is often covered by the organic oil, paste binder and some pollutants, which may block the access of reactants to the graphite particles or attenuate the electron transfer on the surface. Some simple electrochemical surface treatments have been proposed to remove the blocking substances on SPCE, such as pre-anodization [37, 38], electrochemical cycling [39] and oxygen plasma treatment [40]. Surface treatment of the electrode with electrochemical methods can not only remove surface organic contaminants and impurities [37-40], but can possibly adding some oxygenated functionalities, such as CO, O–C–O and O–C O [40]. Electrochemical surface treatment has been demonstrated to be successfully enhanced electrocatalytic activity of electrochemical biosensors [37-41]. The presence of surface oxygenated functionalities may provide adequate micro-space for the

electrode surface at the nano level and may contribute to the increase in electrochemical activity of the electrode [40].

1.4 Diazotization and electro-addressing

Diazotization and coupling reactions are widely applied in chemical industry for organic synthesis, such as in the synthesis of dyes and pigment [42]. It is because diazonium salt exhibits a very lively chemical property and can occur in a variety of reactions and react with a variety of materials. Diazotization reaction is exothermic with a fast reaction rate and, hence, can be carried out under ambient condition. Once the diazonium salt solution is prepared the next experimental procedure should be conducted as soon as possible [43].

Diazonium organic salt has been extensively used for the surface modification. It is not only because of its broad selectivity to wide range of metal and semiconductor materials but also because of its simplicity, efficiency, and speed [44]. Depends on the functional groups it carried, the diazonium organic salt-modified electrode can be functionalized with phenolic, imidazole, or amino group, achieving different types of surface derivatization [45]. The chemistry involved in the diazonium-based surface modification including (i) the diazotation reaction of an aniline derivative to form an aryl diazonium; (ii) generating an aryl radical of this latter species to form a covalent bond to the surface of electrode by the electrochemical reaction. [46]; (iii) the surface of the electrode can be functionalized by functional groups (such as -SH) associated with the diazonium salt [47].

In this thesis, the surface SPCE was first functionalized with carboxylic groups by a layer of 4-aminophenylacetic acid (CMA) through electrochemical deposition. The carboxylic groups on the surface of SPCE were then activated by EDC/NHS. Immediately, gold nanoparticles (AuNPs) or the cysteamine-modified AuNPs were coated on top of the CMA layer by either physical absorption or covalent bonding. The electrochemical properties of CMA-modified, AuNPs-coated SPCE were characterized and analyzed [48].

1.5 Gold nanoparticles (AuNPs) and its applications

Nanotechnology has been widely adopted and integrated with the biosensing technology recently for the detection biomolecules [49]. Nanomaterials, materials with size below 100 nm, have recently attracted eyes of scientists due to their unique optical, electrical and magnetic properties. Silver (Ag) and gold (Au) nanoparticles are two types of metal nanomaterials that have been used in the construction of biosensors due to their unique chemical and physical properties and the surface plasmon resonance (SPR) activity. Gold nanoparticle (AuNP) exhibits its own unique surface plasmon resonance absorption peak [50].

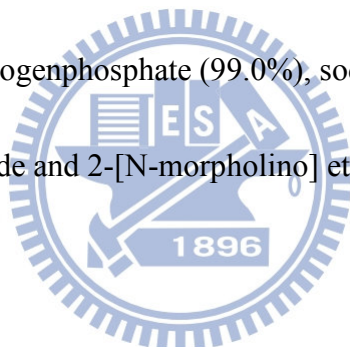
The size of synthesized AuNPs can be controlled in a range of 1-100 nm by the salt concentration and temperature [51, 52]. AuNP has been widely used in numerous areas, such as acting as electron microscopy contrast reagents, mediator of chemical and biochemical sensors, electrical conduction medium, dyes and as catalysts. AuNPs are good bridging substance to link biomolecules, such as enzymes, proteins, and nucleic acids via their surface

charges or via surface functionalization. For example, the negatively charged substances can be associated with AuNPs directly via their surface positive charges. The AuNPs can be easily functionalized through the sulfur-containing linkers. The sulfur can be readily bound to the AuNP surface by a sulfur-Au bond. AuNPs have been used for construction of biosensors because of their excellent ability to immobilize biomolecules to retain the biocatalytic activities of those biomolecules and to enhance the electrochemical redox responses of the biosensors [53]. AuNPs have some fascinating properties, such as favorable micro environment, good biocompatibility and high electron transfer ability (Figure 1), that make them suitable for protein immobilization in biosensors fabrication [54]. In this study the electrocatalytic activity of SPCE after modified by AuNPs with different configurations was investigated. In the first arrangement the SPCE was first modified with a thin layer of cysteamine-coated AuNPs (CNH₂AuNPs), followed by immobilizing the glucose oxidase (GOx) on top of AuNPs, forming a sandwich-like structure. In the second arrangement the SPCE was modified with the mixture of CNH₂AuNPs and GOx. The electrochemical responses of H₂O₂ and glucose on the above enzyme electrodes were then studied [55]. The effect of gold nanoparticles size or surface modification on the electrochemical responses to H₂O₂ was also investigated [56].

2. Materials and Methods

2.1 Materials

Tetrachloroauric (III) acid trihydrate ($\text{HAuCl}_4 \cdot 3\text{H}_2\text{O}$), cysteamine hydrochloride, 4-aminophenylacetic acid (CMA), hydrogen peroxide solution (30%), potassium hexacyanoferrate (III) (approx. 99%), potassium dihydrogenphosphate, bovine serum albumin (BSA) and N-(3-dimethylaminopropyl)-N'-ethylcarbodiimide hydrochloride were purchased from sigma. Glucose oxidase from *Aspergillus niger* was obtained from Sigma. Sodium citrate, sodium nitrate, hydrogen chloride, glucose, sodium chloride (99.5%), potassium chloride (99.5%), disodium hydrogenphosphate (99.0%), sodium dihydrogenphosphate anhydrous, N-hydroxysuccinimide and 2-[N-morpholino] ethanesulfonic acid (99%) were bought from Sigma and Showa.



2.2 Apparatus

A potentiostat CHI 440 (CH Instruments, West Lafayette, IN, USA) connected to a personal computer was used for the measurement of electrochemical responses of biosensors to hydrogen peroxide (H_2O_2). The three-electrode electrochemical system contained a working electrode screen-printed carbon paste electrode (SPCE), a counter electrode (a platinumized electrode) and a reference electrode (Ag/AgCl). The oxygen plasma pre-treatment of the surface of SPCE was performed on Diener electronic (type: Zepto/Atto).

2.3 Preparation of gold nanoparticles (AuNPs)

The preparation of gold nanoparticles was carried out by the conventional Turkevich-Frens citrate reduction method [57]. The double-deionized H₂O (200 mL) in a 500 mL Erlenmeyer flask was first heated to boiling. After boiling, 0.2 mg HAuCl₄ and 0.1 g sodium citrate were added into the flask with gently shaking to allow the chemicals to dissolve. Seal the bottle by a piece of aluminum foil to prevent water evaporation and allow the reaction to proceed until the appearance of the wine-red color (about 10 min). Stop the reaction by putting Erlenmeyer flask on ice for about 10 min. The synthesized gold nanoparticles were characterized by determining absorption peak and the absorbance on the U-3010 spectrophotometer (Hitachi, Japan). The approximate size and the concentration of the synthesized gold nanoparticles can be estimated by the Beer's Law. The AuNPs solution was then stored in an aluminum foil-shield flask in dark at 4°C.

2.4 Preparation of cysteamine-modified AuNPs

The cysteamine (CNH₂)-modified AuNPs (CNH₂AuNPs) was prepared by incubating AuNPs solution and CNH₂ at the final concentration of 10 nM and 0.03 mM, respectively, at room temperature for two hours [58]. The stock CNH₂ solution was prepared by dissolving CNH₂ in d.d. H₂O to a concentration of 20 mM. After incubation the CNH₂AuNPs solution was collected by centrifugation at 13,200 rpm and 4°C for 20 min. After removing supernatant the CNH₂AuNPs pellet was suspended in pH 6.0 phosphate buffer saline (PBS) (137 mM NaCl, 2.7 mM KCl, 10 mM Na₂HPO₄, 1.76 mM KH₂PO₄) containing 0.1% BSA, to prevent

the aggregation. The prepared CNH_2AuNPs solution was then characterized by determining the absorption peak and the absorbance at the peak [59]. The prepared CNH_2AuNPs could be stored at 4°C or used directly.

2.5 Pretreatment and modification of screen-printed carbon paste electrode

Prior to the assembly of three-electrode electrochemical system, the screen-printed carbon paste electrode (SPCE) was pretreated with oxygen plasma under the room temperature at 25 W for 30 sec to increase the hydrophilicity and the electrochemical properties of the SPCE by removing the surface organic pollutants [60]. Subsequently, the electrode was then washed by cyclic voltammetry within the potential range from -1.0 to 1.0 V at a scan rate 100 mV/s [61], followed by immersing in pH 7.0, 1X PBS before the modification. After washing a thin layer of 4-carboxymethyl aryl diazonium (CMA) was electrodeposited on the SPCE. Briefly, 8 mL 4-aminophenylacetic acid in ethanol (30 mM) was mixed with 1 mL HCl (20 mM) and 1 mL NaNO_2 (20 mM) to give the final concentration of 24 mM, 2 mM and 2 mM, respectively. Then the diazonium cation solution was obtained by incubating above mixture in ice-cold water with stirring for 10 min to allow the amino group of the 4-aminophenylacetic acid to be diazoted. In a diazoted 4-aminophenylacetic acid solution (24 mM) the diazonium salt was deposited on the SPCE surface by cyclic voltammetry with the scanning range of -0.7 to 0.8 V and a scan rate of 200 mV/s for 10 cycles. The CMA-modified SPCE was then washed with pH 7.0, 1X PBS, twice and stored at

4°C [62].

2.6 Modification of CMA-coated SPCE with CNH₂AuNPs

The surface of CMA-deposited SPCE (CMA/SPCE) was first activated by cross-linking reagent EDC and NHS before the immobilization of CNH₂AuNPs and GOx [63]. Briefly, the CMA-deposited SPCE was immersed into 0.1 M MES, pH 6.0 buffer solution containing 0.04 mg/mL EDC and 0.06 mg/mL NHS at room temperature for 30 min [64]. After incubation, the surface activated, CMA-deposited SPCE was rinsed once with d.d. H₂O to remove excess unreacted EDC/NHS. Subsequently, 5 μL CNH₂AuNPs solution (0.58 nM) was dropped directly onto the surface of CMA/SPCE. The cross-linking reaction was allowed to be proceeded by placing at room temperature for 30 min first and then staying at 4°C for overnight to form CNH₂AuNP-coated CMA/SPCE electrode (CNH₂AuNP/CMA/SPCE).

2.7 Generation of glucose oxidase electrode

Two types of glucose biosensor was generated and characterized. The first glucose sensor is to immobilize glucose oxidase (GOx) on the CNH₂AuNP/CMA/SPCE (GOx/CNH₂AuNP/CMA/SPCE), forming a sandwich-like structure by cross-linking [65]. The CNH₂ moiety on CNH₂AuNPs allows the immobilization of other biomolecules such as enzymes, antibodies and other protein on the surface of AuNPs [66]. The second glucose biosensor was to immobilize GOx and CNH₂AuNPs mixture on the surface of activated CMA/SPCE (GOx- CNH₂AuNPs/CMA/SPCE). GOx can also interact with the activated

CMA/SPCE to generate GOx/CMA/SPCE, which was used as a control.

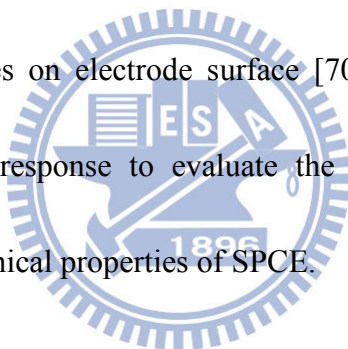
Prior to immobilizing on the CNH₂AuNP/CMA/SPCE or CMA/SPCE, GOx was first activated by mixing 10 μL GOx (184 Units/μL) with 10 μL PBS, pH 6.0 containing 0.04 mg/mL EDC and 0.06 mg/mL NHS under room temperature for 30 min [67]. After activation, GOx (approximate 90 Units) was either mixed with CNH₂AuNP (0.58 nM) in a ratio of 1:1 (v/v) and deposited on the CMA/SPCE [68] or directly deposited on the CNH₂AuNP/CMA/SPCE. The cross-linking reaction was allowed to proceed at room temperature for 30 min, followed by incubating at 4°C overnight to form covalent bonding.

Two types of GOx electrodes were constructed. The first is GOx- CNH₂AuNPs/CMA/SPCE, a glucose sensor with GOx and CNH₂AuNPs mixture immobilizing on the CMA/SPCE. The second one is GOx/CNH₂AuNPs/CMA/SPCE, a glucose sensor with GOx immobilizing on the CNH₂AuNPs/CMA/SPCE.

2.8 Cyclic voltammetry and electrochemical measurements

Cyclic voltammetry (CV) was widely used to characterize the electrochemical properties of electrodes. CV is a powerful method for qualitative or quantitative analysis of the electrochemical reactions. The experiment was usually performed on the conventional three-electrode electrochemical system. The working electrode is supplied with a linearly changed potential to trigger the corresponding electrochemical responses or currents, which would be subsequently recorded and analyzed [69].

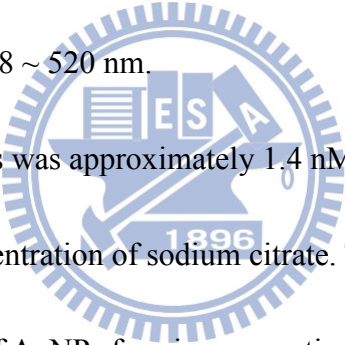
Cyclic voltammetry was also adopted to clean the surface of electrode by the redox reactions. The cyclic voltammetry for either electrode cleaning or electrochemical analysis of H_2O_2 was performed in PBS, pH 7.0 with a scanning range between -1.0 and +1.0 V and a scanning rate of 100 mV/s for 5 to 10 cycles. Current-time responses of H_2O_2 on AuNPs-coated SPCE or glucose on glucose sensors were carried out in PBS, pH 7.0 at the fixed voltage of +0.7 V, followed by monitoring the electric redox current signals of electrodes. It is worth to know that the measurement of electrochemical response of reactant should not be carried out until resting current reached steady state. Current-time responses can be used to evaluate the changes on electrode surface [70]. In this thesis, we used cyclic voltammetry and current-time response to evaluate the effect of different AuNPs-based modifications on the electrochemical properties of SPCE.



3. Results and Discussion

3.1 Generation and characterization of gold nanoparticles

AuNPs could be synthesized by Turkevich-Frens citrate reduction method [71] and characterized by determining the visible light absorbance spectra between the wavelengths of 700 nm and 400 nm. The particle size and the concentration of AuNPs could be determined via their peak wavelength and peak absorbance. The concentration of AuNPs could be calculated based on the Beer's law ($A = \epsilon\lambda bc$). Where, $\epsilon\lambda$ equals to $1.25 \times 10^9 \text{ cm}^{-1} \text{ M}^{-1}$ for 20 nm AuNP solution with O.D. of 1.0. The generated AuNP under 2 mM sodium citrate exhibited a peak absorption at 518 ~ 520 nm.



The concentration of AuNPs was approximately 1.4 nM. Interestingly, the particle size of AuNPs was affected by the concentration of sodium citrate. The negatively charged citrate ions may coated on the surface of AuNPs forming a negatively charged layer. Hence, AuNPs are more prone to rejection and difficult to attract each other, resulting in the formation of gold nanoparticles smaller particle size [72].

When surface modified, the absorbance and the color of colloidal AuNPs changed markedly. This phenomenon will be used to characterize the surface-functionalized AuNPs.

3.2 Generation and characterization of cysteamine-AuNPs

Cysteamine (CNH_2) contains a sulfhydryl group (-SH), which is relative active and is readily oxidized to form disulfide bonds or to form a covalent bond with various metals,

especially gold, under room temperature. The modification of AuNP with CNH₂ may functionalize its surface with amine groups. However, when generating CNH₂-coated AuNPs (CNH₂AuNP) under the high concentration of CNH₂ the aggregation of AuNPs may be increased due to the hydrophobic property of the CNH₂ under the neutral condition. The amine group of CNH₂ has a dissociation constant of around 10 making it nearly neutral under pH 7.0. To prevent the possible occurrence of aggregation and precipitation of CNH₂AuNP different ratios of AuNPs and CNH₂ was prepared and incubated at room temperature for two hours. As shown in Figure 3, when the mole ratio of CNH₂ to AuNPs was 2500:1 the generated CNH₂AuNPs exhibited the pink color with the absorption peak of 522 ~ 524 nm; whereas, when the mole ratio increased to 3000:1 the generated CNH₂AuNPs exhibited the purple color with the absorption peak of 526 ~ 535 nm. Further study was performed by determining the absorption peak and absorbance of the generated CNH₂AuNPs. The AuNPs without modification exhibited an absorption peak at 518 nm. The CNH₂AuNPs synthesized under the condition with CNH₂ and AuNPs in a mole ratio of 2500:1 exhibited an absorption peak of 524 nm (Figure 4) with estimated particle size of 20 nm. In comparison, the CNH₂AuNPs synthesized under the condition with CNH₂ and AuNPs in a mole ratio of 3000:1 exhibited an absorption peak of 535 nm (Figure 5) with estimated particle size of 50 nm. Apparently, the aggregation between the CNH₂AuNPs might occur under the higher mole ratio of CNH₂ and AuNPs. Accordingly, the mole ratio of CNH₂ to AuNPs at 3000:1 was

adopted for the production of CNH₂AuNPs, which exhibited the absorbance peak at 526 nm (CNH₂ and AuNPs concentration increased tenfold) and the concentration of 0.6 nM. The particle size of CNH₂AuNP also depends on the reaction time between the CNH₂ and AuNPs. The size of CNH₂AuNPs is larger with longer reaction time. Therefore, the reaction time of 2 hours was set for the generation of CNH₂AuNPs.

3.3 Preparation of diazonium salt-coated SPCE

In this study the aryl diazonium was used as the linker for the immobilization of AuNPs and enzymes. Prior to the aryl diazonium modification the surface of SPCE was treated with oxygen plasma under the condition of 25 W for 30 sec, followed by cyclic voltammetric treatment within the scanning range of -1.0 ~ 1.0 V and scanning rate of 100 mV/s for 10 cycles. The surface cleaning with oxygen plasma may remove surface impurities and lead to increasing hydrophilicity of the electrode surface [58]. The electrochemical reaction could be facilitated after surface cleaning.

The electrodeposition of diazoted CMA on the surface of SPCE was performed by immersing oxygen plasma-cleaned SPCE in CMA stock solution (Figure 7) and run cyclic voltammetric scanning within the range of -0.7 and +0.8 V at a scan rate of 200 mV/s. After electrodeposition the CMA-coated SPCEs were immersed in pH 7, PBS buffer and stored at 4°C before use (Figure 8).

The CMA-electrodeposited SPCE was characterized by the pH-dependency of the

electrochemical responses. The pKa of the acryl carboxylic acids (-COOH) is probably around 4-5. Hence the CMA-deposited SPCE exhibited a pH-dependent electrochemical response to $[\text{Fe}(\text{CN})_6]^{3-}$ due to the differential ionic status of CMA under different pH values. It is neutral under pH 2.0 and negatively charged at pH 7.0. With bare SPCE the cyclic voltammograms of 1 mM $\text{K}_3[\text{Fe}(\text{CN})_6]$ in pH 2.0 and pH 7.0, PBS buffers were similar (Figure 9A), suggesting no pH-dependent effect. However, with CMA-modified SPCE the cyclic voltammograms of 1 mM $\text{K}_3[\text{Fe}(\text{CN})_6]$ in pH 2.0 exhibited clear redox peaks at 0.15 V and 0.3 V (Figure 9B, red line); whereas, at pH 7.0 the redox peaks of the cyclic voltammogram were almost invisible (Figure 9A, blue line). This result suggests that the redox reactions of $[\text{Fe}(\text{CN})_6]^{3-}$ in pH 7.0, PBS buffer were largely abolished presumably due to the repelling effect of the negatively charged CMA group to the anionic ion $[\text{Fe}(\text{CN})_6]^{3-}$ at pH 7.0.

3.4 Characterization of AuNP-modified CMA/SPCE

The modification of CMA/SPCE with AuNPs and CNH_2AuNPs was illustrated in Figure 10. The CNH_2AuNP contains an amine group (- NH_2), which is helpful for the immobilization of other substances. The electrochemical properties of the AuNP- or CNH_2AuNP -modified SPCE were determined by their electrochemical responses to H_2O_2 . The cyclic voltammetry of bare SPCE, CMA/SPCE, AuNP/CMA/SPCE and $\text{CNH}_2\text{AuNP/CMA/SPCE}$ without H_2O_2 was shown in Figure 11. The basal responses of SPCE increased with the modification of

AuNP and CNH₂AuNP.

The electrochemical responses of bare SPCE, CMA/SPCE, AuNP/CMA/SPCE and CNH₂AuNP/CMA/SPCE to 500 μM H₂O₂ were also determined (Figure 12). The electrochemical current of SPCE to H₂O₂ was also increase following the modification of AuNP and CNH₂AuNP. The current-time responses of bare SPCE, CMA/SPCE, AuNP/CMA/SPCE and CNH₂AuNP/CMA/SPCE to H₂O₂ were 3.97×10^{-8} , 4.36×10^{-8} , 7.05×10^{-8} , 7.18×10^{-8} A/500 μM H₂O₂ (Figure 13). This result suggests that gold nanoparticles or modified gold nanoparticles could significant increase electrochemical responses. The Figure 14 shows the does-current response of bare SPCE, CMA/SPCE, AuNP/CMA/SPCE and CNH₂AuNP/CMA/SPCE to various concentration of H₂O₂. The sensitivity of bare SPCE, CMA/SPCE, AuNP/CMA/SPCE and CNH₂AuNP/CMA/SPCE to H₂O₂ was 7.94×10^{-6} , 8.72×10^{-6} , 1.41×10^{-5} , 1.44×10^{-5} A/cm²/mM (Figure 15), respectively.

The effect of particle size of AuNPs (40 nm and 50 nm) in the electrochemical responses to H₂O₂ was further studied (Figure 16). As shown in Figure 16, the larger of the AuNP (50 nm) exhibited higher electrochemical response to H₂O₂ (7.28×10^{-5} A / cm² / mM H₂O₂) than that of smaller AuNPs (40 nm) (6.6×10^{-5} A / cm² / mM H₂O₂), suggesting that electrochemical responses of SPCE also affects electrochemical response.

3.5 Development and characterization of GOx electrode

In this thesis, two types of glucose biosensors were developed using AuNP-coated SPCE:

(i) the CMA/SPCE coated with the mixture of GOx and CNH₂AuNPs, termed GOx-CNH₂AuNP/CMA/SPCE (Figure 17A) and (ii) CMA/SPCE was sequentially coated with CNH₂AuNPs and GOx to generate the GOx/CNH₂AuNPs/CMA/SPCE (Figure 17B). The CNH₂AuNPs-modified and GOx-CMA/SPCE electrodes were used as controls. In comparison the GOx-CMA/SPCE, GOx-CNH₂AuNP/CMA/SPCE and GOx/CNH₂AuNPs/CMA/SPCE exhibited the electrochemical response to 0.5 mM glucose of 8.12×10^{-7} , 9.88×10^{-7} , 1.44×10^{-6} A/cm²/mM glucose, respectively (Figure 19). This result suggests that GOx/CNH₂AuNPs/CMA/SPCE exhibited a response higher than that of GOx-CNH₂AuNPs/CMA/SPCE [73]. The sensitivity of GOx-CMA/SPCE, GOx-CNH₂AuNP/CMA/SPCE and GOx/CNH₂AuNPs/CMA/SPCE to glucose was 8.12×10^{-7} , 9.88×10^{-7} , 1.44×10^{-6} A/cm²/mM, respectively. The dose-current response of electrodes to glucose was performed under different concentrations of glucose (0.5, 1, 1.5 and 2 mM) (Figure 18). The result showed that the GOx/CNH₂AuNPs/CMA/SPCE was better than that of other two GOx electrodes. There was no responses to glucose on the CNH₂AuNPs/CMA/SPCE (data not shown).

4. Conclusion

In this thesis, different surface modifications of SPCE with AuNPs were generated and characterized. First, 4-(aminophenyl)acetic acid was adopted as a linker to modify SPCE. Subsequently, AuNP and GOx with different configuration were deposited on the surface of CMA/SPCE. The SPCE modified with AuNPs exhibited higher electrochemical responses to hydrogen peroxide (500 μM) than that of bare SPCE. The sensitivity of SPCE, AuNP/SPCE and $\text{CNH}_2\text{AuNP/SPCE}$ was 7.94×10^{-6} , 1.41×10^{-5} , $1.44 \times 10^{-5} \text{ A/cm}^2/\text{mM}$, respectively. This result shows that AuNPs enhance the responses to hydrogen peroxide significantly.

Glucose biosensor was developed by immobilizing the GOx on the AuNP-modified SPCE. Two classes of glucose sensors were synthesized in this study. One is the deposition of GOx and AuNPs mixture on the CMA/SPCE and the other is putting the GOx on top of AuNP layer. Interestingly, the sensitivity of $\text{GOx-CNH}_2\text{AuNPs mix/CMA/SPCE}$ to glucose ($1.44 \times 10^{-6} \text{ A/cm}^2/\text{mM}$) was shown to be relatively higher than that of $\text{GOx/CNH}_2\text{AuNPs/CMA/SPCE}$ ($9.88 \times 10^{-7} \text{ A/cm}^2/\text{mM}$).

5. Reference

1. Grieshaber, D., MacKenzie, R., Vörös, J. and Reimhult, E. (2008) Electrochemical Biosensors – Sensor Principles and Architectures. *Sensors* 8, 1400-1458.
2. Rodriguez-Mozaz, S., Lopez de Alda, M.J., Barceló, D. (2006) Biosensors as useful tools for environmental analysis and monitoring. *Anal Bioanal Chem* 386, 1025-1041.
3. Omidfar, K., Khorsand, F., Darziani Azizi, M. (2013) New analytical applications of gold nanoparticles as label in antibody based sensors. *Biosensors and Bioelectronics* 43, 336-347.
4. Ahirwal, G.K., Mitra, C.K. (2010) Gold nanoparticles based sandwich electrochemical immunosensor. *Biosensors and Bioelectronics* 25, 2016-2020.
5. Kerman, K., Saito, M., Yamamura, S., Takamura, Y., Tamiya, E. (2008) Nanomaterial-based electrochemical biosensors for medical applications. *Trends in Analytical Chemistry* 27, 585-592.
6. Eker, S., Kargi, F. (2007) Performance of a hybrid-loop bioreactor system in biological treatment of 2, 4, 6-tri-chlorophenol containing synthetic wastewater: Effect of hydraulic residence time. *Journal of Hazardous Materials* 144, 86-92.
7. Bagni, G., Osella, D., Sturchio, E., Mascini, M. (2006) Deoxyribonucleic acid (DNA) biosensors for environmental risk assessment and drug studies. *Analytica Chimica Acta* 573-574, 81-89.

8. Wei, Y., Brandazza, A., Pelosi, P. (2008) Binding of polycyclic aromatic hydrocarbons to mutants of odorant-binding protein: A first step towards biosensors for environmental monitoring. *Biochimica et Biophysica Acta* 1784, 666-671.
9. Perez-Lopez, B., Merkoci, A. (2011) Nanomaterials based biosensors for food analysis applications. *Trends in Food Science and Technology* 22, 625-639.
10. Tothill, I.E. (2001) Biosensors developments and potential applications in the agricultural diagnosis sector. *Computers and Electronics in Agriculture* 30, 205-218.
11. Duveneck, G.L., Pawlak, M., Neuschäfer, D., Bär, E., Budach, W., Pieleś, U., Ehrat, M. (1997) Novel bioaffinity sensors for trace analysis based on luminescence excitation by planar waveguides. *Sensors and Actuators B* 38-39, 88-95.
12. Marazuela, M.D., Moreno-Bondi, M.C. (2002) Fiber-optic biosensors – an overview. *Anal Bioanal Chem* 372, 664-682.
13. Sadik, O.A., Yan, F. (2007) Electrochemical biosensors for monitoring the recognition of glycoprotein-lectin interactions. *Analytica Chimica Acta* 588, 292-296.
14. Narakathu, B.B., Atashbar M.Z., Bejcek, B.E. (2010) Improved detection limits of toxic biochemical species based on impedance measurements in electrochemical biosensors. *Biosensors and Bioelectronics* 26, 923-928.
15. Lv, Y.Y., Wu, J., Xu, Z.K. (2010) Colorimetric and fluorescent sensor constructing from the nanofibrous membrane of porphyrinated polyimide for the detection of hydrogen

- chloride gas. *Sensors and Actuators B* 148, 233-239.
16. Nguyen-Hgoc, H., Tran-Minh, C. (2007) Fluorescent biosensor using whole cells in an inorganic translucent matrix. *Analytica Chimica Acta* 583, 161-165.
 17. McGrath, T.F., Andersson, K., Campbell, K., Fodey, T.L., Elliott, C.T. (2013) Development of a rapid low cost fluorescent biosensor for detection of food contaminants. *Biosensors and Bioelectronics* 41, 96-102.
 18. Carlucci, L., Favero, G., Tortolini, C., Fusco, M.D., Romagnoli, E., Minisola, S., Mazzei, F. (2013) Several approaches for vitamin D determination by surface plasmon resonance and electrochemical affinity biosensors. *Biosensors and Bioelectronics* 40, 350-355.
 19. Lan, Y.B., Wang, S.Z., Yin, Y.G., Hoffmann, W.C., Zheng, X.Z. (2008) Using a Surface Plasmon Resonance Biosensor for Rapid Detection of Salmonella Typhimurium in Chicken Carcass. *Journal of Bionic Engineering* 5, 239-246.
 20. Azzam, E.M.S., Bashir, A., Shekhah, O., Alawady, A.R.E., Birkner, A., Grunwald, Ch., Woll, Ch. (2009) Fabrication of a surface plasmon resonance biosensor based on gold nanoparticles chemisorbed onto a 1, 10-decanedithiol self-assembled monolayer. *Thin Solid Films* 518,387-391.
 21. Chung, J.W., Kim, S.D., Bernhardt, R., Pyun, J.C. (2005) Application of SPR biosensor for medical diagnostics of human hepatitis B virus (hHBV). *Sensors and Actuators* 111-112, 416-422.

22. Harbon, U., Xie, B., Venkatesh, R., Danielsson, B. (1997) Evaluation of a miniaturized thermal biosensor for the determination of glucose in whole blood. *Clinica Chimica Acta* 267, 225-237.
23. Kwak, B.S., Kim, H.O., Kim, J.H., Lee, S., Jung, H.I. (2012) Quantitative analysis of sialic acid on erythrocyte membranes using a photothermal biosensor. *Biosensors and Bioelectronics* 35, 484-488.
24. Rigobello, M.P., Folda, A., Scutari, G., Bindoli, A. (2005) The modulation of thiol redox state affects the production and metabolism of hydrogen peroxide by heart mitochondria. *Archives of Biochemistry and Biophysics* 441, 112-122.
25. Loo, A.E.K., Halliwell, B. (2012) Effects of hydrogen peroxide in keratinocyte-fibroblast co-culture model of wound healing. *Biochemical and Biophysical Research Communications* 423, 253-258.
26. Díaz-Llera, S., Podlutzky, A., Österholm, A.M., Hou, S.M., Lambert, B. (2000) Hydrogen peroxide induced mutations at the HPRT locus in primary human T-lymphocytes. *Mutation Research* 469, 51-61.
27. Silva, R.A.B., Montes, R.H.O., Richter, E.M., Munoz, R.A.A. (2012) Rapid and selective determination of hydrogen peroxide residues in milk by batch injection analysis with amperometric detection. *Food Chemistry* 133, 200-204.
28. Desesso, J.M., Lavin, A.L., Hsia, S.M. and Mavis, R.D. (2000) Assessment of the

- carcinogenicity associated with oral exposures to hydrogen peroxide. *Food and Chemical Toxicology* 38, 1021-1041.
29. Behl, C. (1999) Alzheimer's Disease and Oxidative Stress: Implications for Novel Therapeutic Approaches. *Progress in Neurobiology* 57, 301-323.
30. Yang, W., Li, Y., Bai, Y., Sun, C. (2006) Hydrogen peroxide biosensor based on myoglobin/colloidal gold nanoparticles immobilized on glassy carbon electrode by Nafion film. *Sensors and Actuators B* 115, 42-48.
31. Owens, D.S., Parker, P.Y., and Benton, D. (1997) Blood Glucose and Subjective Energy Following Cognitive Demand. *Physiology and Behavior* 62, 471-478.
32. Gamburgzev, S., Atanasov, P., Ghindilis, A.L., Wilkins, E. (1997) Bifunctional hydrogen peroxide electrode as an amperometric transducer for biosensors. *Sensors and Actuators B* 43, 70-77.
33. Lee, D.Y., Park, S.H., Qian, D.J., Kwon, Y.S. (2009) Electrochemical detection of hydrogen peroxide via hemoglobin-DNA/pyterpy-modified gold electrode. *Current Applied Physics* 9, e232-e234.
34. Wang, J., Tian, B., Nascimento, V.B. and Angnes, L. (1998) Performance of screen-printed carbon electrodes fabricated from different carbon inks. *Electrochimica Acta* 43, 3459-3465.
35. Lee, S.H., Fang, H.Y., Chen, W.C., Lin, H.M., Chang, C.A. (2005) Electrochemical

- study on screen-printed carbon electrodes with modification by iron nanoparticles in Fe(CN)₆⁴⁻/Fe(CN)₆³⁻ redox system. *Anal Bioanal Chem* 383, 532-538.
36. Hart, J.P., Crew, A.P., Crouch, E., Honeychurch, K.C., and Pemberton, M. (2004) Some Recent Designs and Developments of Screen-Printed Carbon Electrochemical Sensors/Biosensors for Biomedical, Environmental, and Industrial Analyses. *Analytical Letters* 37, 789-830.
37. Engstrom, R.C. (1982) Electrochemical pretreatment of glassy carbon electrodes. *Anal. Chem.* 54, 2310-2314.
38. Cui, G., Yoo, J.H., Lee, J.S., Yoo, J., Uhm, J.H., Cha, G.S. and Nam, H. (2001) Effect of pre-treatment on the surface and electrochemical properties of screen-printed carbon paste electrodes. *Analyst* 126, 1399-1403.
39. Wang, J., Naser, N., Angnes, L., Wu, H. and Chen, L. (1992) Metal-Dispersed Carbon Paste Electrodes. *Anal. Chem.* 64, 1285-1288.
40. Wang, S.C., Chang, K.S., Yuan, C.J. (2009) Enhancement of electrochemical properties of screen-printed carbon electrodes by oxygen plasma treatment. *Electrochimica Acta* 54, 4937-4943.
41. Suffredini, H.B., Pedrosa, V.A., Codognoto, L., Machado, S.A.S., Rocha-Filho, R.C., Avaca, L.A. (2004) Enhanced electrochemical response of boron-doped diamond electrodes brought on by a cathodic surface pre-treatment. *Electrochimica Acta* 49,

4021-4026.

42. Noroozi-Pesyan, N., Khalafy, J., Malekpoor, Z. (2009), Diazotization of Aniline Derivatives and Diazo Couplings in the Presence of p-Toluenesulfonic Acid by Grinding. *Prog. Color Colorants Coat*, 2, 61-70
43. Sreekumar, N.V., Narayana, B., Hegde, P., Manjunatha, B.R., Sarojini, B.K. (2003) Determination of nitrite by simple diazotization method. *Microchemical Journal* 74, 27-32.
44. Dabbagh, H.A., Teimouri, A., Najafi Chermahini, A. (2007) Green and efficient diazotization and diazo coupling reactions on clays. *Dyes and Pigments* 73, 239-244.
45. Li, F., Feng, Y., Dong, P., Tang, B. (2010) Gold nanoparticles modified electrode via a mercapto-diazoaminobenzene monolayer and its development in DNA electrochemical biosensor. *Biosensors and Bioelectronics* 25, 2084-2088.
46. Corgier, B.P., Marquette, C.A. and Blum, L.J. (2005) Diazonium-Protein Adducts for Graphite Electrode Microarrays Modification: Direct and Addressed Electrochemical Immobilization. *J. Am. Chem. Soc.* 127, 18328-18332.
47. Jiang, W., Yuan, R., Chai, Y., Mao, L., Su, H. (2011) A novel electrochemical immunoassay based on diazotization-coupled functionalized bioconjugates as trace labels for ultrasensitive detection of carcinoembryonic antigen. *Biosensors and Bioelectronics* 26, 2786-2790.

48. Morita, K., Yamaguchi, A., Teramae, N. (2004) Electrochemical modification of benzo-15-crown-5 ether on a glassy carbon electrode for alkali metal cation recognition. *Journal of Electroanalytical Chemistry* 563, 249-255.
49. Knopp, D., Tang, D., Niessner, R. (2009) Review: Bioanalytical application of biomolecule-functionalized nanometer-sized doped silica particles. *Analytica Chimica Acta* 647, 14-30.
50. Tao, A.R., Habas, S. and Yang, P. (2008) Shape Control of Colloidal Metal Nanocrystals. *Small* 4, 310-325.
51. Tiwari, P.M., Vig, K., Dennis, V.A. and Singh, S.R. (2011) Functionalized Gold Nanoparticles and Their Biomedical Application. *Nanomaterials* 1, 31-63.
52. Liu, F.K., Wei, G.T. (2004) Effect of Mobile-Phase Additives on Separation of Gold Nanoparticles by Size-Exclusion Chromatography. *Chromatographia* 59, 115-119.
53. Du, Y., Luo, X.L., Xu, J.J., Chen, H.Y. (2007) A simple method to fabricate a chitosan-gold nanoparticles film and its application in glucose biosensor. *Bioelectrochemistry* 70, 342-347.
54. Fan, L., Zhao, G., Shi, H., Liu, M., Li, Z. (2013) A highly selective electrochemical impedance spectroscopy-based aptasensor for sensitive detection of acetamiprid. *Biosensors and Bioelectronics* 43, 12-18.
55. Grosan, C.B., Varodi, C., Vulcu, A., Olenic, L., Pruneanu, S., Almasan, V. (2012)

- Structural and electrochemical characterization of novel leucine-gold nanoparticles modified electrode. *Electrochimica Acta* 63, 146-152.
56. Matveeva, E.G., Shtoyko T., Gryczynski, I., Akopova, I., Gryczynski, Z. (2008) Fluorescence quenching/enhancement surface assays: Signal manipulation using silver-coated gold nanoparticles. *Chemical Physics Letters* 454, 85-90.
57. Kimling, J., Maier, M., Okenve, B., Kotaidis, V., Ballot, H. and Plech, A. (2006) Turkevich Method for Gold Nanoparticles Synthesis Revisited. *J. Phys. Chem. B* 110, 15700-15707.
58. Zhang, M., Liu, Y.Q. and B Ye, B.C. (2011) Colorimetric assay for sulfate using positively-charged gold nanoparticles and its application for real-time monitoring of redox process. *Analyst* 136, 4558-4562.
59. Gao, J., Huang, X., Liu, H., Zan, F., Ren, J. (2012) Colloidal Stability of Gold Nanoparticles Modified with Thiol Compounds: Bioconjugation and Application in Cancer Cell Imaging. *Langmuir* 28, 4464-4471.
60. Chang, Y.H., Hsu, C.L., Yuan, C.J., Tang, S.F., Chiang, H.J., Jang, H.D., Chang, K.S. (2011) Improvement of the inter-electrode reproducibility of screen-printed carbon electrodes by oxygen plasma etching and an image color level method for quality control. *Materials Science and Engineering C* 31, 1265-1270.
61. Morrin, A., Killard, A.J. and Smyth, M.R. (2003) Electrochemical Characterization of

- Commercial and Home-Made Screen-Printed Carbon Electrodes. *Analytical Letters* 36, 2021-2039.
62. Mülazimoğlu, A.D. and Mercimek, B. (2012) Electrochemical Grafting by Reduction of 4-Methylaminobenzenediazonium Salt at GC, Au and Pt Electrode: Investigation of Sensitivity Against Phenol by Cyclic Voltammetry. *Anal Bioanal Electrochem* 4, 327-341.
63. Liu, G., Luais, E. and Gooding, J.J. (2011) The Fabrication of Stable Gold Nanoparticle-Modified Interfaces for Electrochemistry. *Langmuir* 27, 4176-4183.
64. Polsky, R., Harper, J.C., Wheeler, D.R., Dirk, S.M., Arango, D.C., Brozik, S.M. (2008) Electrically addressable diazonium-functionalized antibodies for multianalyte electrochemical sensor applications. *Biosensors and Bioelectronics* 23, 757-764.
65. Zhang, S., Wang, N., Niu, Y., Sun, C. (2005) Immobilization of glucose oxidase on gold nanoparticles modified Au electrode for the construction of biosensor. *Sensors and Actuators B* 109, 367-374.
66. Sharma, A., Matharu, Z., Sumana, G., Solanki, R., Kim, C.G., Malhotra, B.D. (2010) Antibody immobilized cysteamine functionalized-gold nanoparticles for aflatoxin detection. *Thin Solid Films* 519, 1213-1218.
67. Li, D., He, Q., Cui, Y., Duan, L., Li, J. (2007) Immobilization of glucose oxidase onto gold nanoparticles with enhanced thermostability. *Biochemical and Biophysical*

- Research Communications 355, 488-493.
68. Zhang, H., Meng, Z., Wang, Q., Zheng, J. (2011) A novel glucose biosensor based on direct electrochemistry of glucose oxidase incorporated in biomediated gold nanoparticles-carbon nanotubes composite film. *Sensors and Actuators B* 158, 23-27.
69. Evans, D.H., O'Connell, K.M., Petersen, R.A. and Kelly, M.J. (1983) Cyclic Voltammetry. *Journal of Chemical Education* 60, 290-293.
70. Zhou, H., Chen, H., Luo, S., Chen, J., Wei, W., Kuang, Y. (2004) Preparation and bioelectrochemical responses of the poly (*m*-phenylenediamine) glucose oxidase electrode. *Sensors and Actuators B* 101, 224-230.
71. Liu, Z., Zu, Y., Guo, S. (2009) Synthesis of micro-scale gold nanochains by a modified citrate reduction method. *Applied Surface Science* 255, 5827-5830.
72. Krishnamurthy, S., Yun, Y.S. (2013) Recovery of microbially synthesized gold nanoparticles using sodium citrate and detergents. *Chemical Engineering Journal* 214, 253-261.
73. Ramanaviciene, A., Nastajute, G., Snitka, V., Kausaite, A., German, N., Barauskas-Memenas, D., Ramanavicius, A. (2009) Spectrophotometric evaluation of gold nanoparticles as redox mediator for glucose oxidase. *Sensors and Actuators B* 137, 483-489.
74. Saha, K., Agasti, S.S., Kim, C., Li, X. and Rotello, V.M. (2012) Gold Nanoparticles in

Chemical and Biological Sensing. Chem. Rev. 112, 2739-2779.



Figures

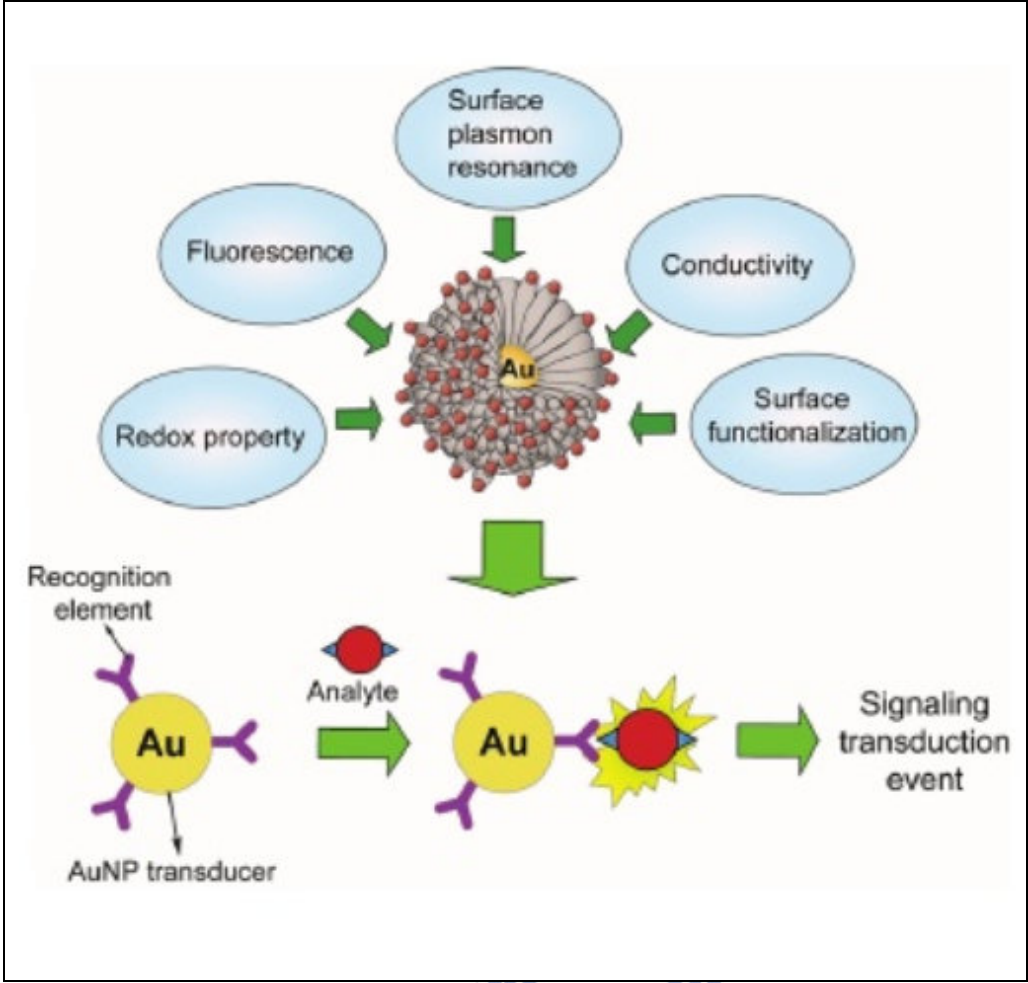


Figure 1. The surface modification and applications of gold nanoparticles [74].

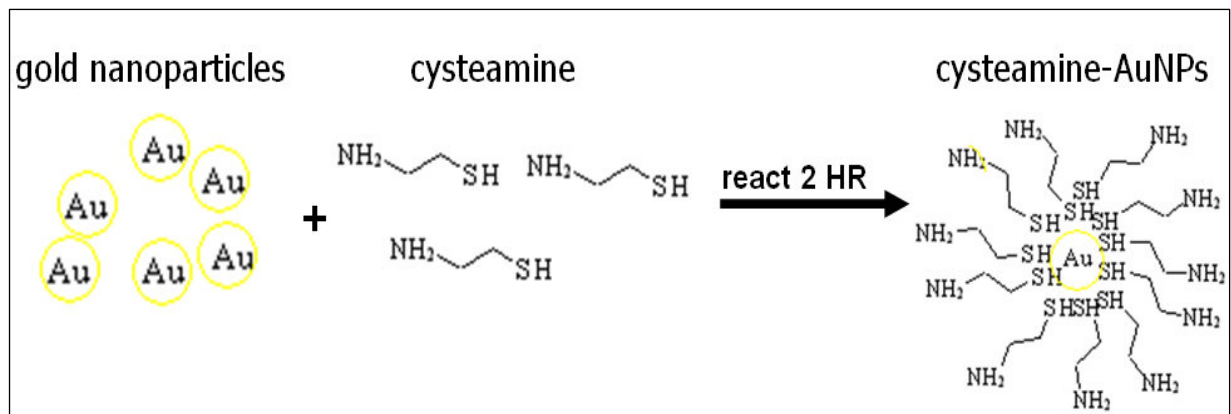


Figure 2. Diagram of the modification of AuNPs with cysteamine. Sulfur can spontaneously form a covalent bond with Au.



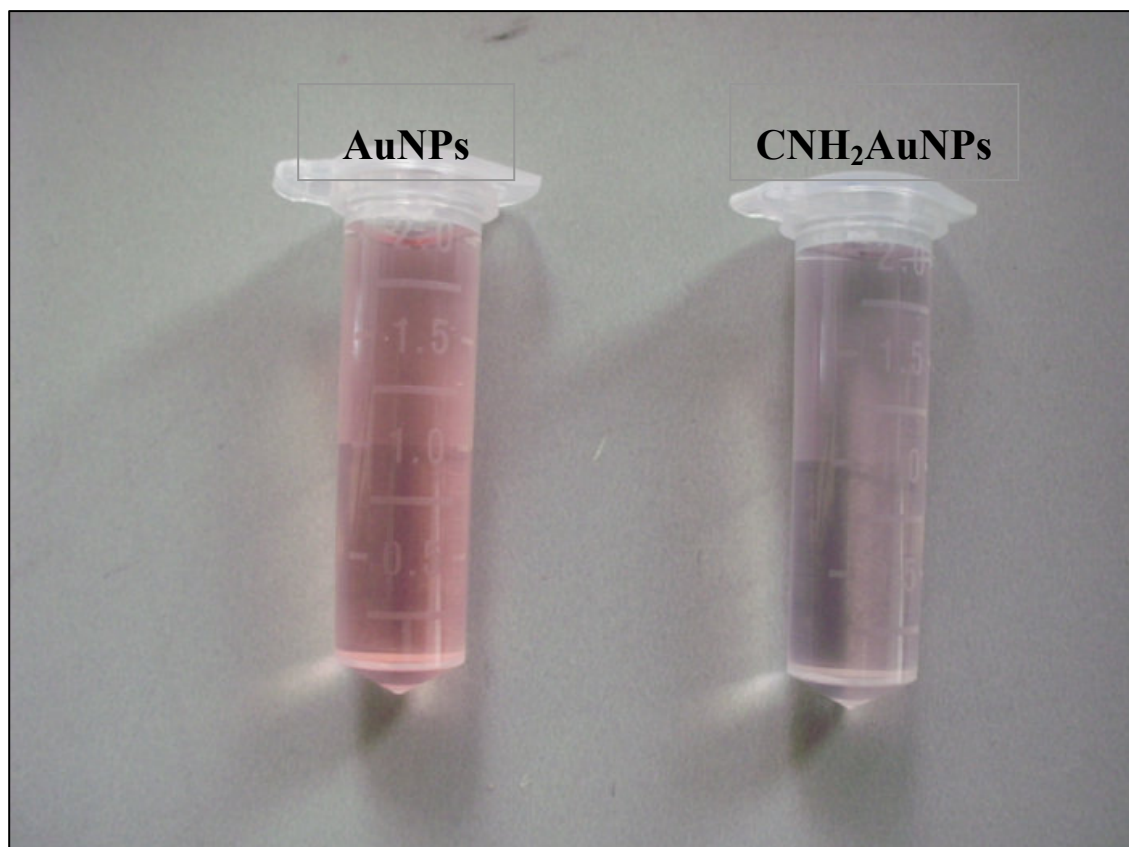


Figure 3. The appearance of the synthesized AuNP colloidal with or without surface modification of cysteamine. The AuNP solution exhibited pink color; while the CNH₂-modified AuNPs exhibited purple color.

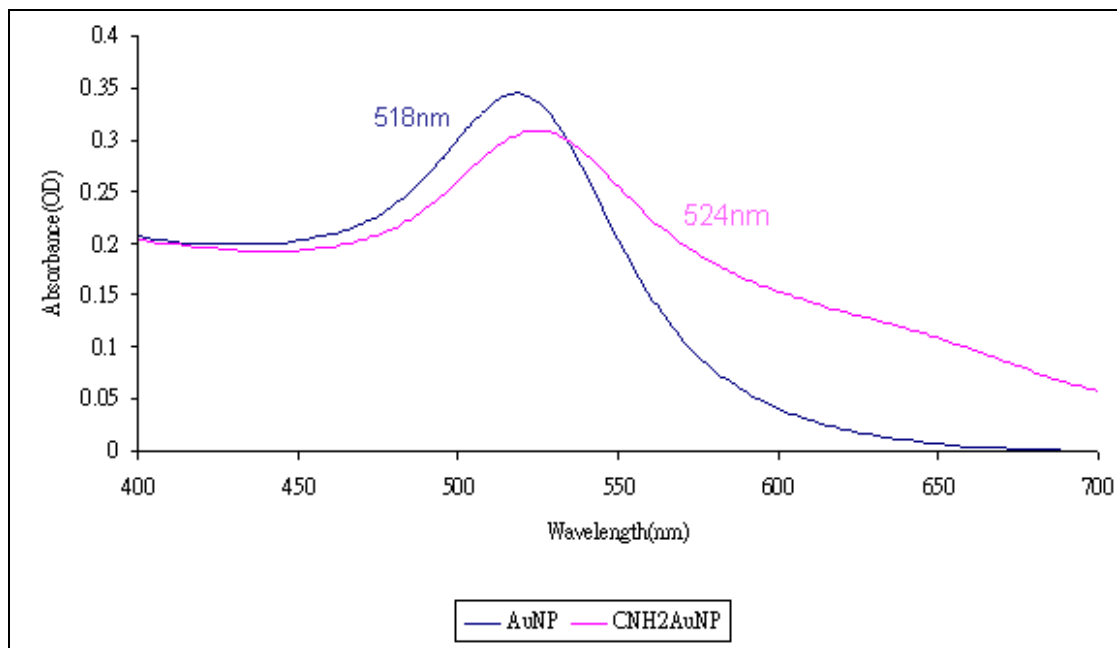
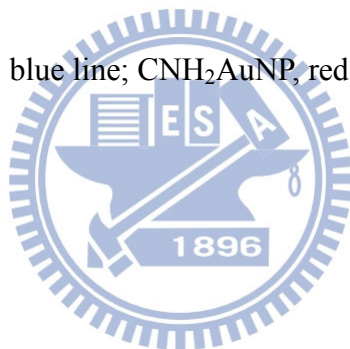


Figure 4. Wavelength scanning of AuNP and CNH₂-modified AuNPs within wavelengths between 400 and 700 nm. AuNP, blue line; CNH₂AuNP, red line.



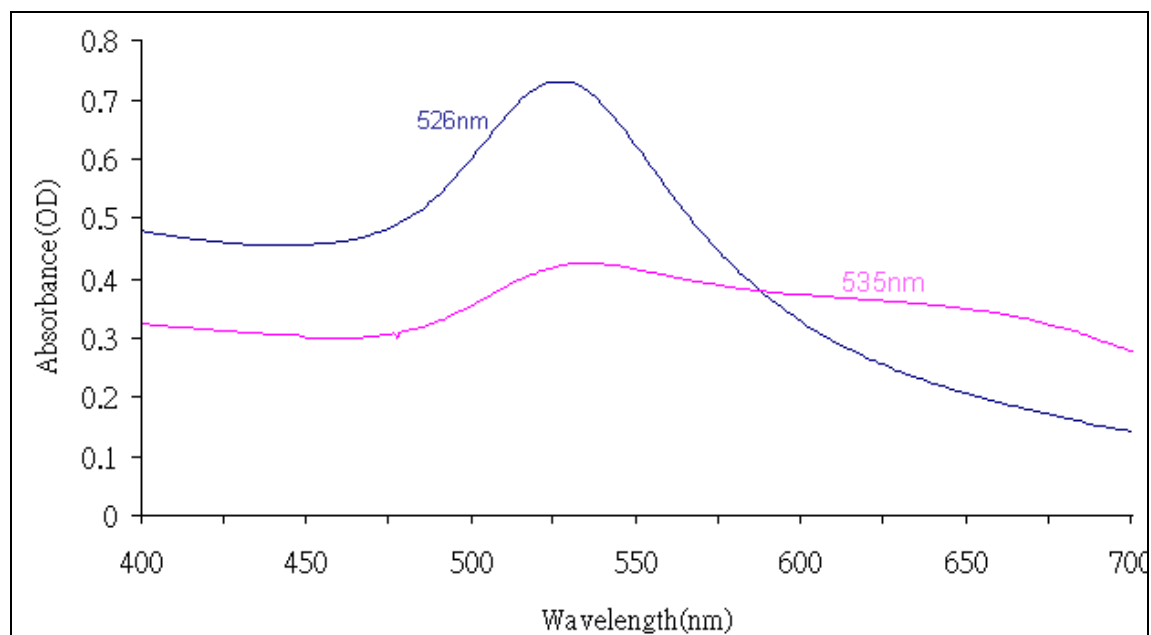
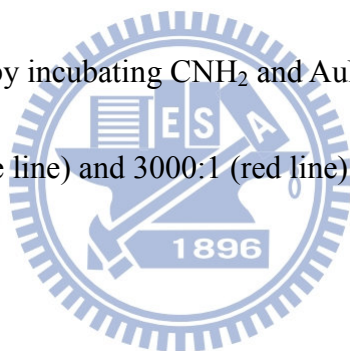


Figure 5. Wavelength scanning of AuNPs with different level of CNH₂ modification. The CNH₂AuNPs were synthesized by incubating CNH₂ and AuNPs in a micro-centrifuge tube with a mole ratio of 2500:1 (blue line) and 3000:1 (red line) at room temperature for 2 hours.



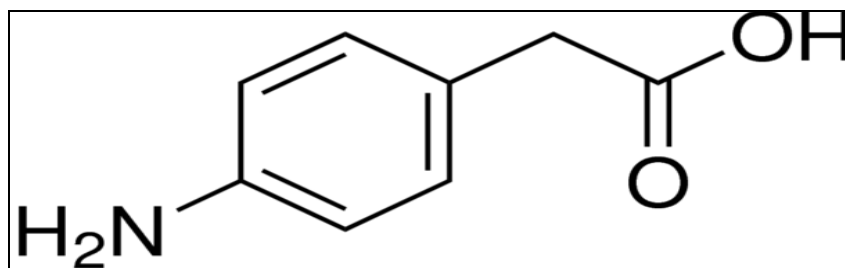


Figure 6. Chemical structure of aniline derivatives 4-(aminophenyl)acetic acid.



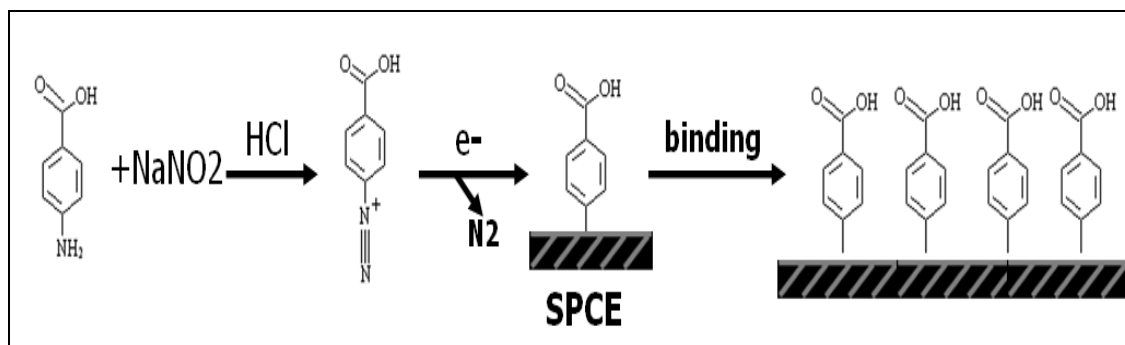


Figure 7. Simple diagram of diazotization and coupling reactions. 4-(aminophenyl)acetic acid (CMA) was first diazotated by reacting with HCl and NaNO_2 . After reaction, the diazonium salt was coupled to the surface of SPCE by cyclic voltammetry.



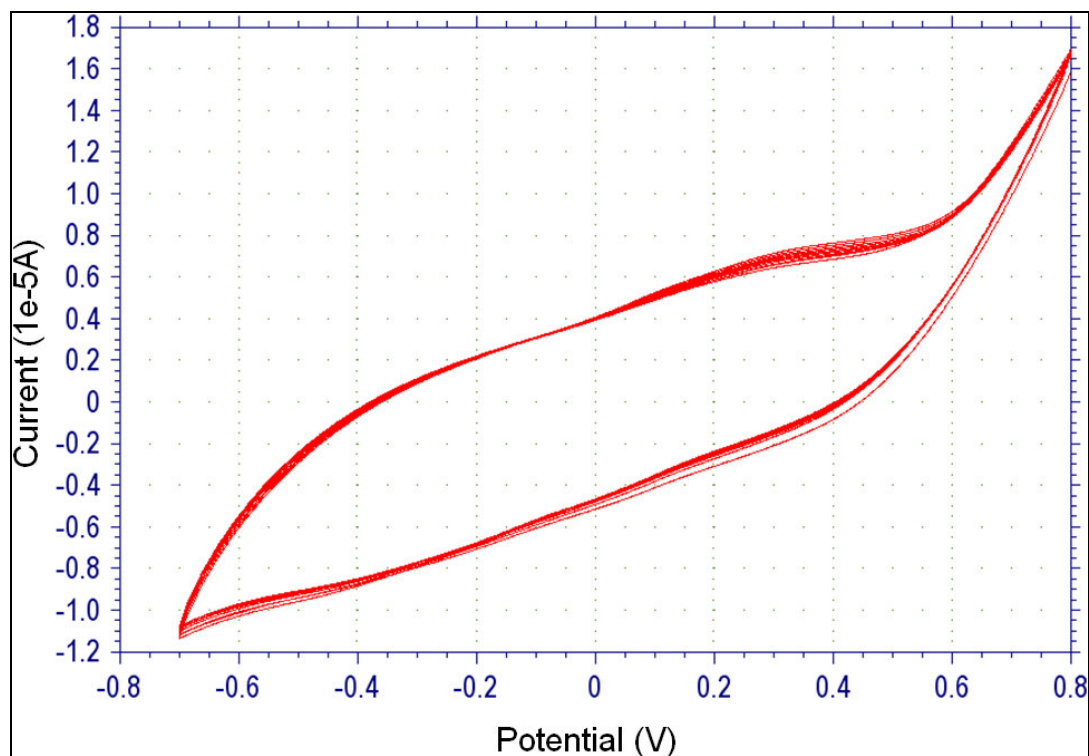


Figure 8. Electrodeposition of diazonium salt on the surface of SPCE by cyclic voltammetry.

The electrodeposition of diazonium salt was performed by dipping plasma-treated SPCE in 4-(aminophenyl)acetic acid solution (24 mM), followed by cyclic voltammetry within the range of -0.7 V and +0.8 V at the scanning rate of 200 mV/s for 5 ~ 10 cycles.

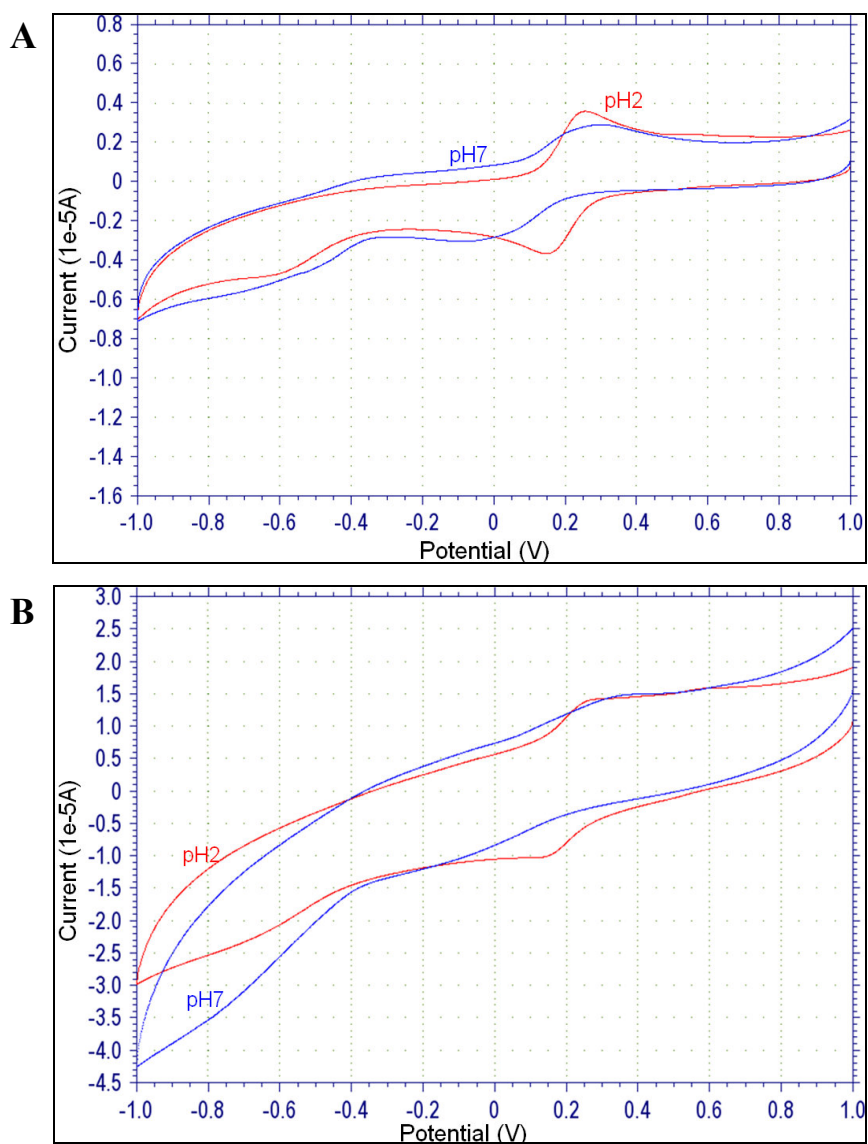


Figure 9. Cyclic voltammetry of 1 mM $K_3[Fe(CN)_6]$ in pH 2.0 or pH 7.0 PBS. The cyclic voltammograms of bare SPCE (A), and the diazonium salt-deposited SPCE (B) at pH 2.0 (red line) and pH 7.0 (blue line).

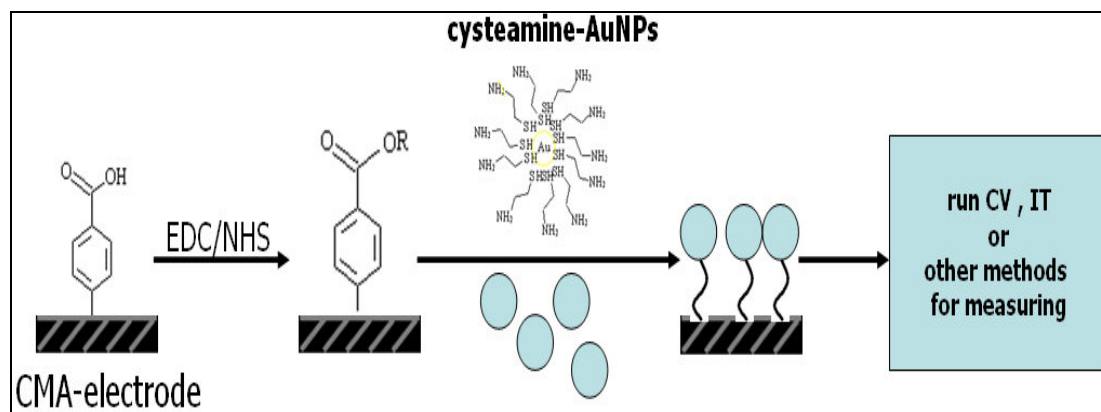
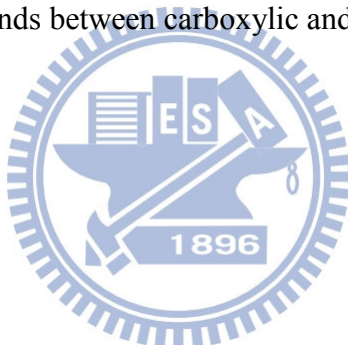


Figure 10. Activation and modification of amine group of CMA on the SPCE for the immobilization of AuNPs. EDC and NHS were used to activate the carboxylic group of CMA on the SPCE. Subsequently, CNH_2AuNPs solution was dropped onto the surface of activated CMA/SPCE to form covalent bonds between carboxylic and amine groups.



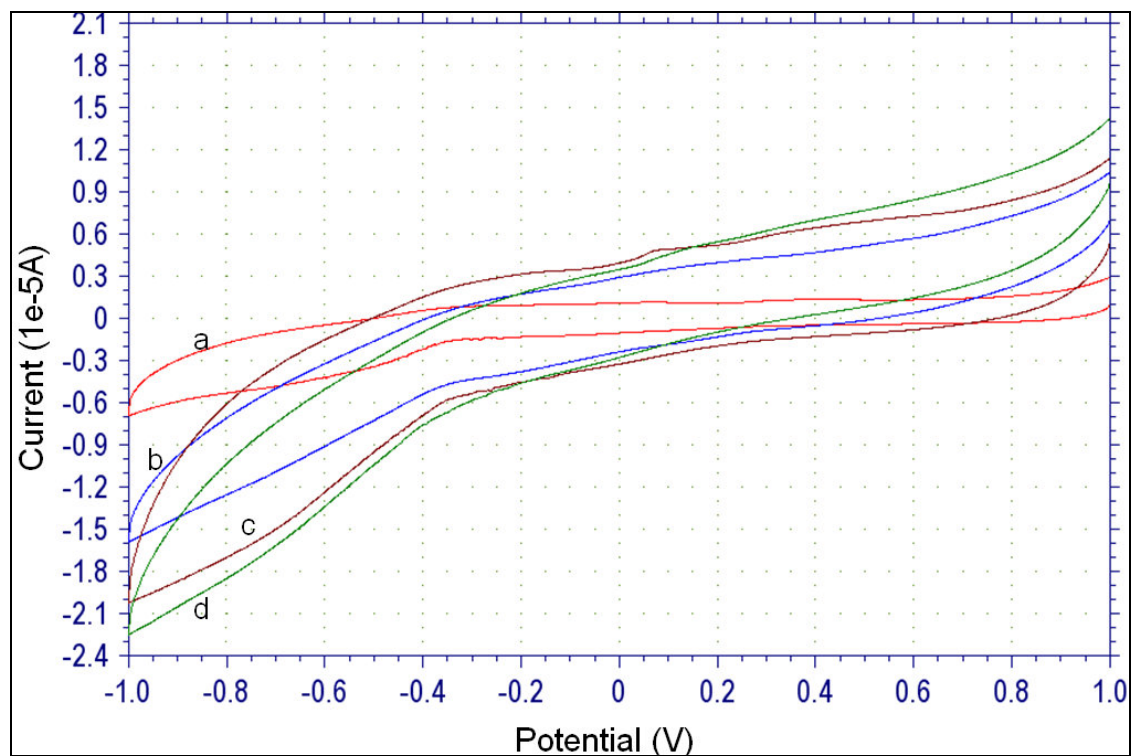
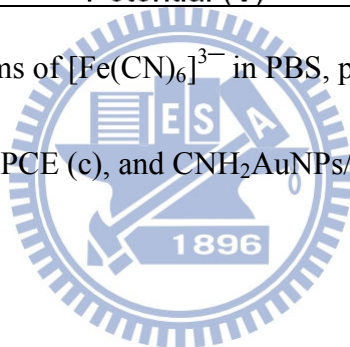


Figure 11. Cyclic voltammograms of $[\text{Fe}(\text{CN})_6]^{3-}$ in PBS, pH 7.0 on bare SPCE (a), CMA/SPCE (b), AuNPs/CMA/SPCE (c), and $\text{CNH}_2\text{AuNPs}/\text{CMA}/\text{SPCE}$ (d).



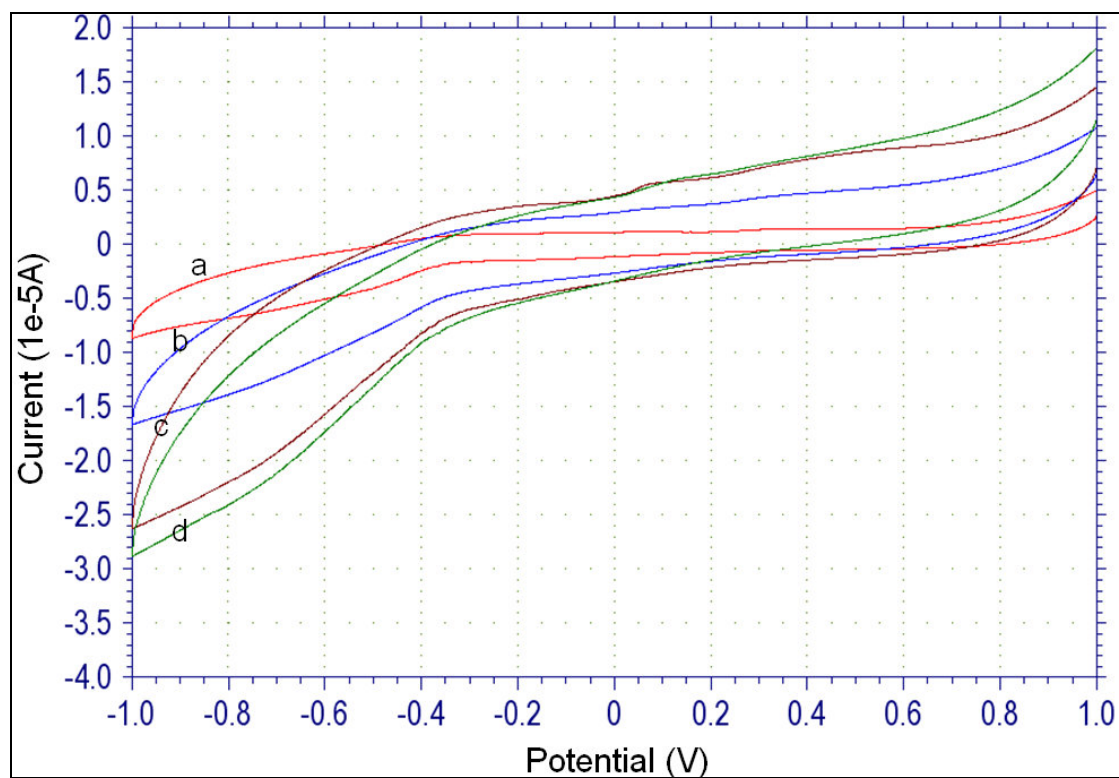
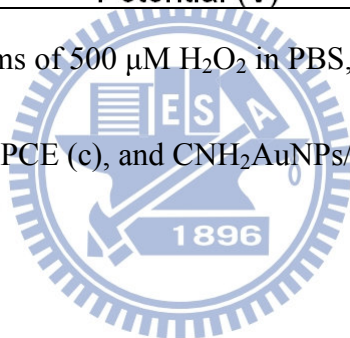


Figure 12. Cyclic voltammograms of 500 μM H_2O_2 in PBS, pH 7.0 on bare SPCE (a), CMA/SPCE (b), AuNPs/CMA/SPCE (c), and CNH_2AuNPs /CMA/SPCE (d).



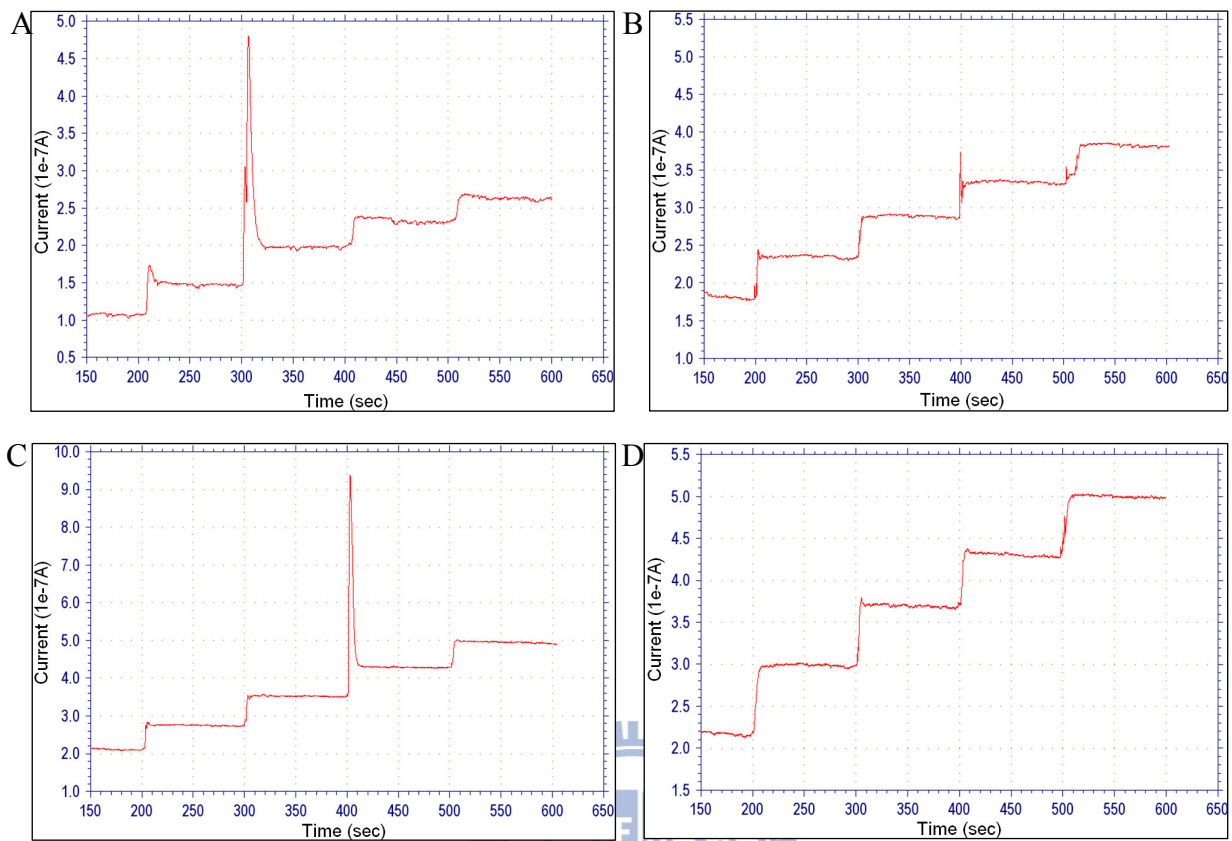


Figure 13. Current-time response of on SPCE and modified SPCE. Step response curve of bare SPCE (A), CMA/SPCE (B), AuNPs/CMA/SPCE (C) and CNH₂AuNPs/CMA/SPCE (D) to 500 μM H₂O₂ were performed in PBS, pH 7.0. Working potential was +0.7 V vs. Ag/AgCl.

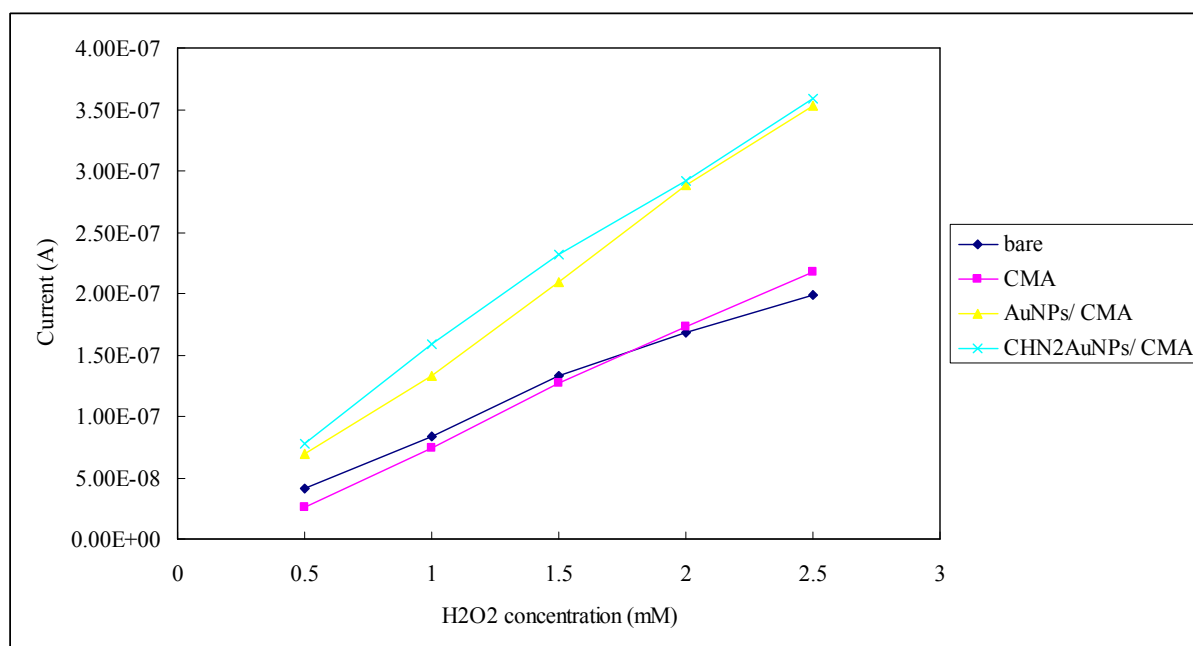
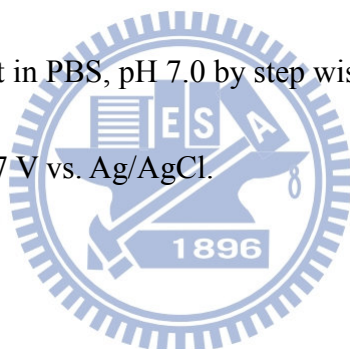


Figure 14. Dose response of SPCE and modified SPCE to H₂O₂. The measurement of the response to H₂O₂ was carried out in PBS, pH 7.0 by step wisely adding 500 μM H₂O₂ at each time. Working potential was +0.7 V vs. Ag/AgCl.



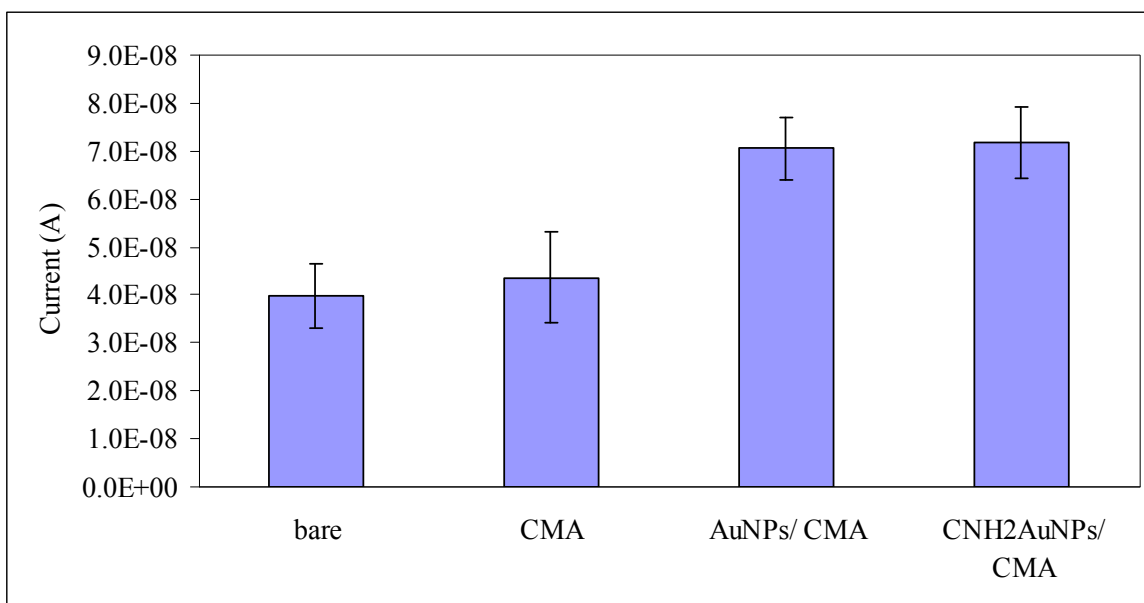


Figure 15. Electrochemical response of bare SPCE, CMA/SPCE, AuNP/ CMA/SPCE and CNH₂AuNPs/CMA/SPCE to 500 μ M H₂O₂. The measurement was performed in PBS, pH 7.0.



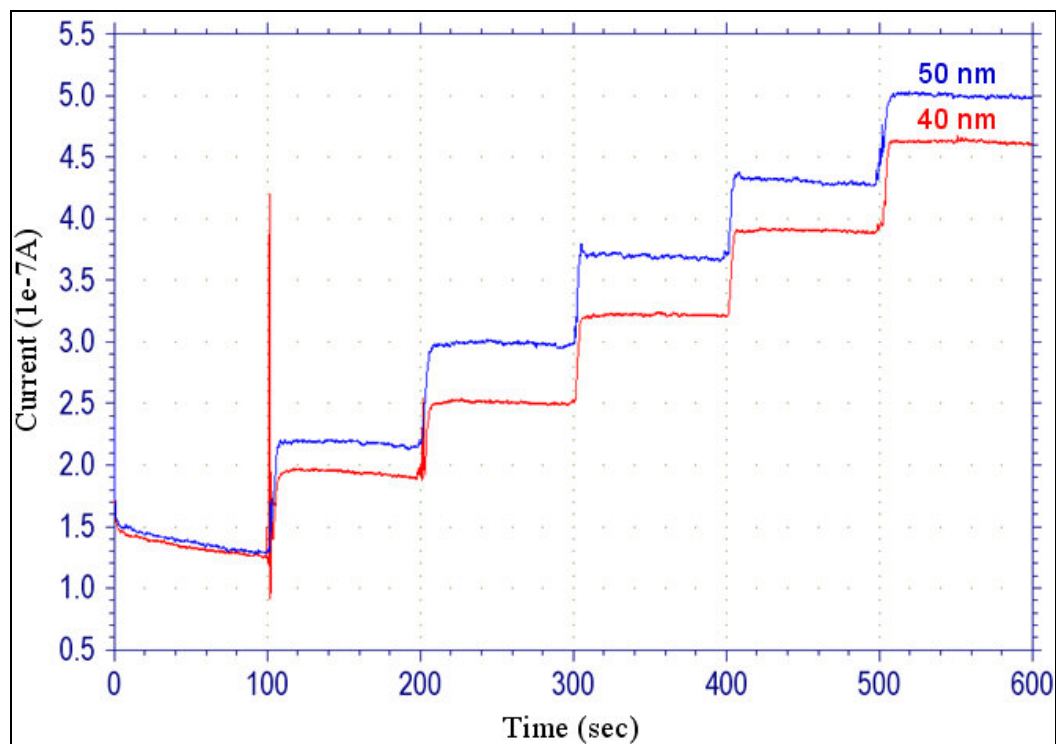


Figure 16. Current-time response curves of CNH₂AuNPs/CMA/SPCE. The step responses of CNH₂AuNPs/CMA/SPCE to 500 μM H₂O₂ in PBS, pH 7.0. Working potential was +0.7 V vs. Ag/AgCl.

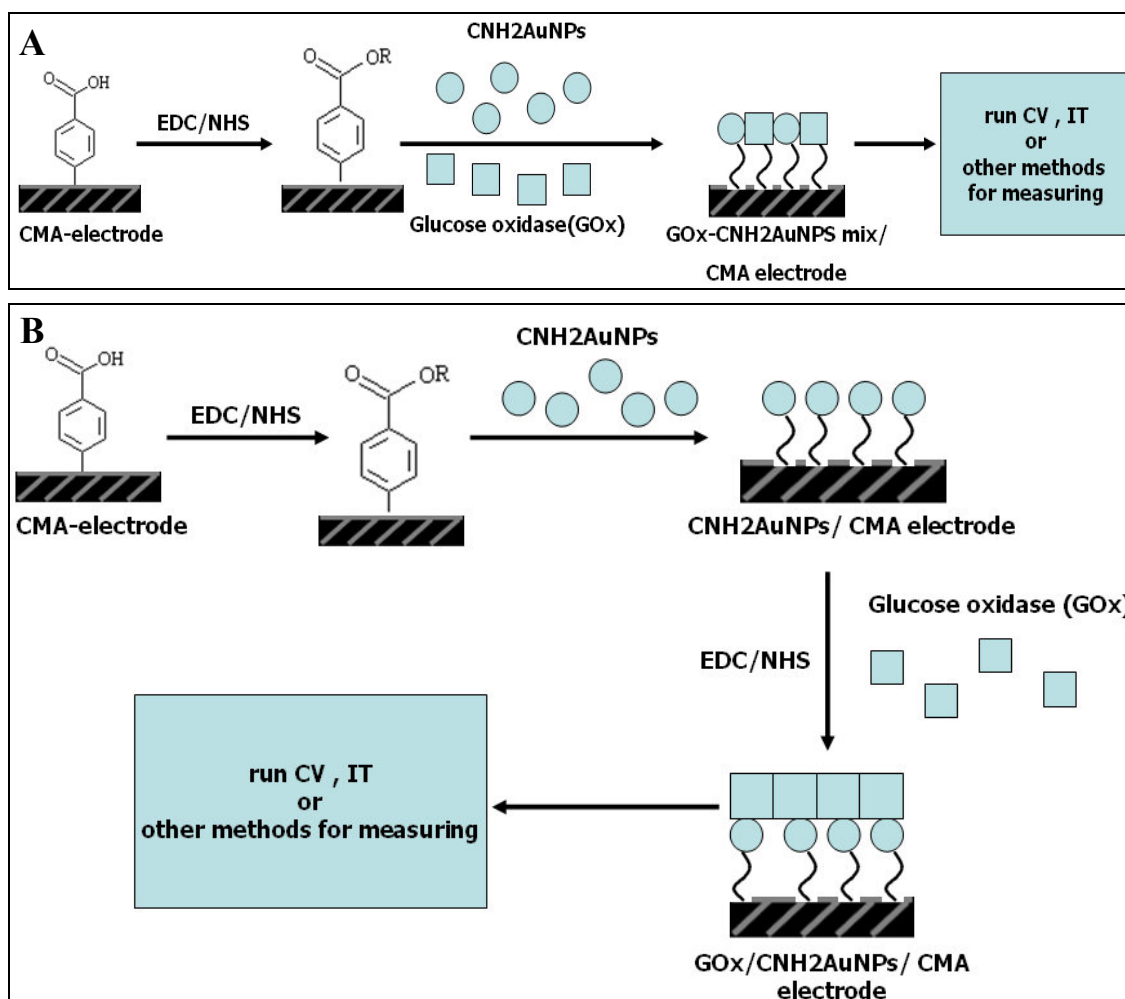


Figure 17. Simple diagrams of the construction of glucose biosensors. (A) GOx-CNH₂AuNPs mix/CMA/SPCE was constructed by covalently link the GOx and CNH₂AuNPs mixture on the : EDC/NHS activated CMA/SPCE. (B) The construction of GOx/CNH₂AUNPs/CMA/SPCE was carried out by first coating CNH₂AuNPs on the EDC/NHS activated CMA/SPCE, followed by immobilizing the EDC/NHS-activated GOx on top of CNH₂AUNPs/CMA/SPCE.

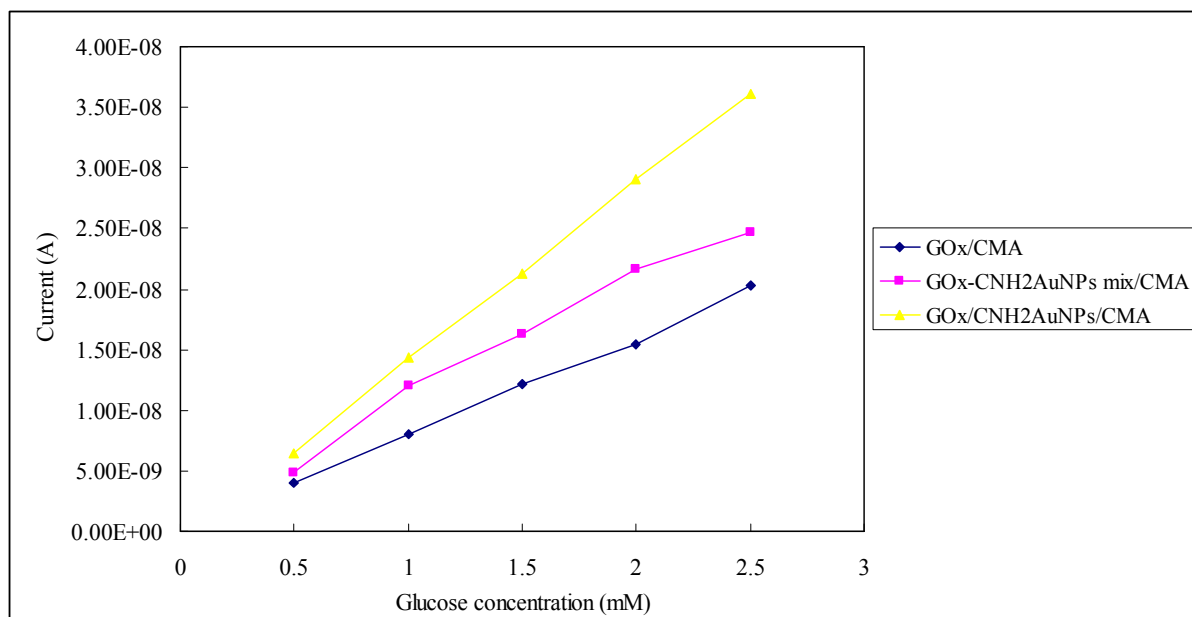
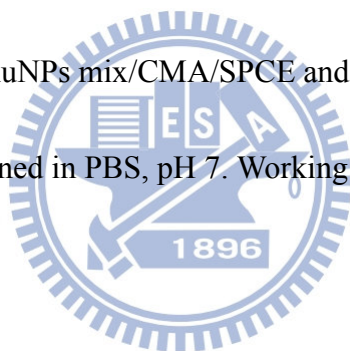


Figure 18. Dose responses of the developed glucose biosensors to glucose. The responses of GOx/CMA/SPCE, GOx-CNH₂AuNPs mix/CMA/SPCE and GOx/CNH₂AuNPs/CMA/SPCE to 500 μ M glucose were determined in PBS, pH 7. Working potential was +0.7 V vs. Ag/AgCl.



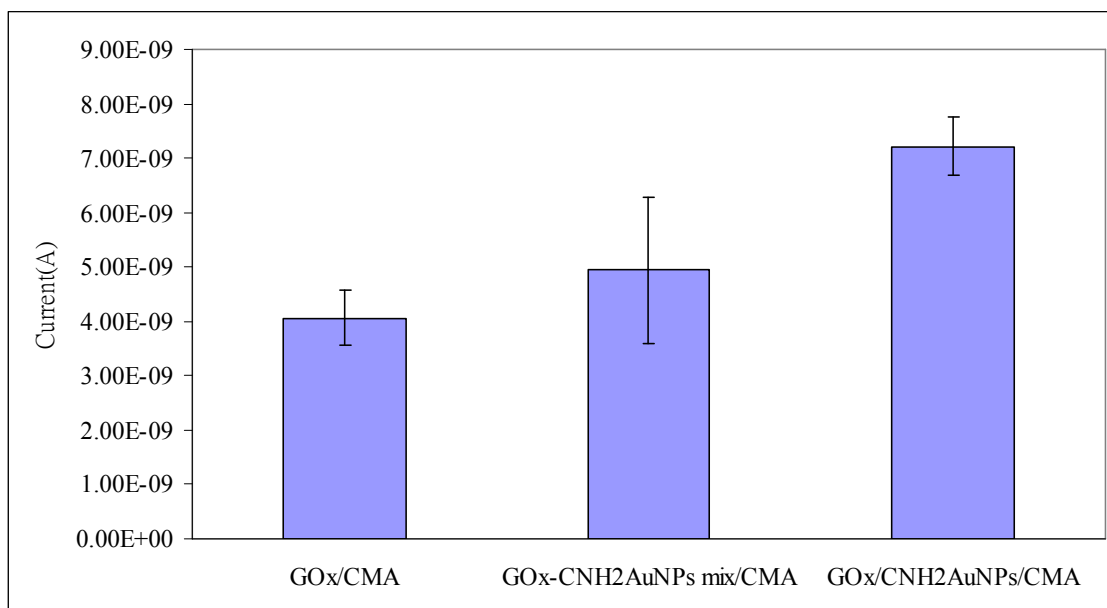


Figure 19. Sensitivity of GOx/CMA/SPCE, GOx-CNH₂AuNPs mix/CMA/SPCE and GOx/CNH₂AuNPs/CMA/SPCE to 500 μ M glucose. The measurement was performed in PBS, pH 7.0. Working potential was +0.7 V vs. Ag/AgCl.

